**Table 1.** Multiple Genotype Infection rate per locus of the *P. vivax* population in South Korea.

| Locus | No. of MGI isolates | MGI rate (%) |
|---|---|---|
| MS1 | 9 | 10.3 |
| MS4 | 52 | 59.8 |
| MS5 | 6 | 6.9 |
| MS6 | 3 | 3.4 |
| MS7 | 73 | 83.9 |
| MS8 | 35 | 40.2 |
| MS9 | 10 | 11.5 |
| MS12 | 38 | 43.7 |
| MS15 | 0 | 0.0 |
| MS20 | 27 | 31.0 |
| Average | 25.3 | 29.1 |

MGI: Multiple genotype infection. Sample size: 87 isolates.
doi:10.1371/journal.pntd.0001592.t001

genetic diversity was reassessed for each group. For the first group, the averages ± SE of $A$ and $H_E$ were 2.70±0.26 and 0.36±0.06, respectively. For the second group, the averages ± SE of $A$ and $H_E$ were 3.80±0.57 and 0.50±0.10, respectively (Fig. 1). The levels of genetic diversity were relatively higher in the second group, with $P$ values at 0.11 and 0.24 for average $A$ and average $H_E$, respectively.

Furthermore, we also divided the population into 3 groups, each covering 5-year periods: 1994 to 1998 (33 isolates), 1999 to 2003 (36 isolates) and 2004 to 2008 (18 isolates). The level of genetic diversity was reassessed for each group (Fig. 3). For the first group, the averages ± SE of $A$ and $H_E$ were 2.50±0.27 and 0.31±0.05, respectively. For the second group, the averages ± SE of $A$ and $H_E$ were 3.00±0.42 and 0.42±0.09, respectively. For the third group, the averages ± SE of $A$ and $H_E$ were 3.80±0.57 and 0.56±0.10, respectively. The levels of genetic diversity gradually increased with $P$ values at 0.06 and 0.05 if we compared the difference of the average $A$ between the first group (1994–1998) and the third group (2003–2008) and the difference of the average $H_E$ between the first and the third group, respectively.

## Multilocus linkage disequilibrium (LD)

Likewise, the analysis of genetic diversity, $I_A^S$ values were also calculated for the two populations: one comprised the isolates collected from 1994 to 2000 and the other comprised the isolates collected from 2001 to 2008, with permutation testing of the null hypothesis of $I_A^S = 0$ (equilibrium of multilocus frequencies) (Table 3). When the single-clone haplotype was used in the analysis, the $I_A^S$ values of the former (1994–2000) and the latter (2001–2008) were 0.529 and 0.218, respectively, whereas when the unique haplotypes were used in the analysis, those of the former and the latter were 0.346 and 0.173, respectively. Significant linkage disequilibrium was observed in both populations ($P<0.001$).

Similar to the analyses of genetic diversity, we also divided the population into 3 groups covering 5-year periods: 1994 to 1998 (33 isolates), 1999 to 2003 (36 isolates) and 2004 to 2008 (18 isolates). The $I_A^S$ values were also calculated for each group. When the single-clone haplotype was used in the analysis, the $I_A^S$ values of the first (1994–1998), the second (1999–2003) and the third (2004–

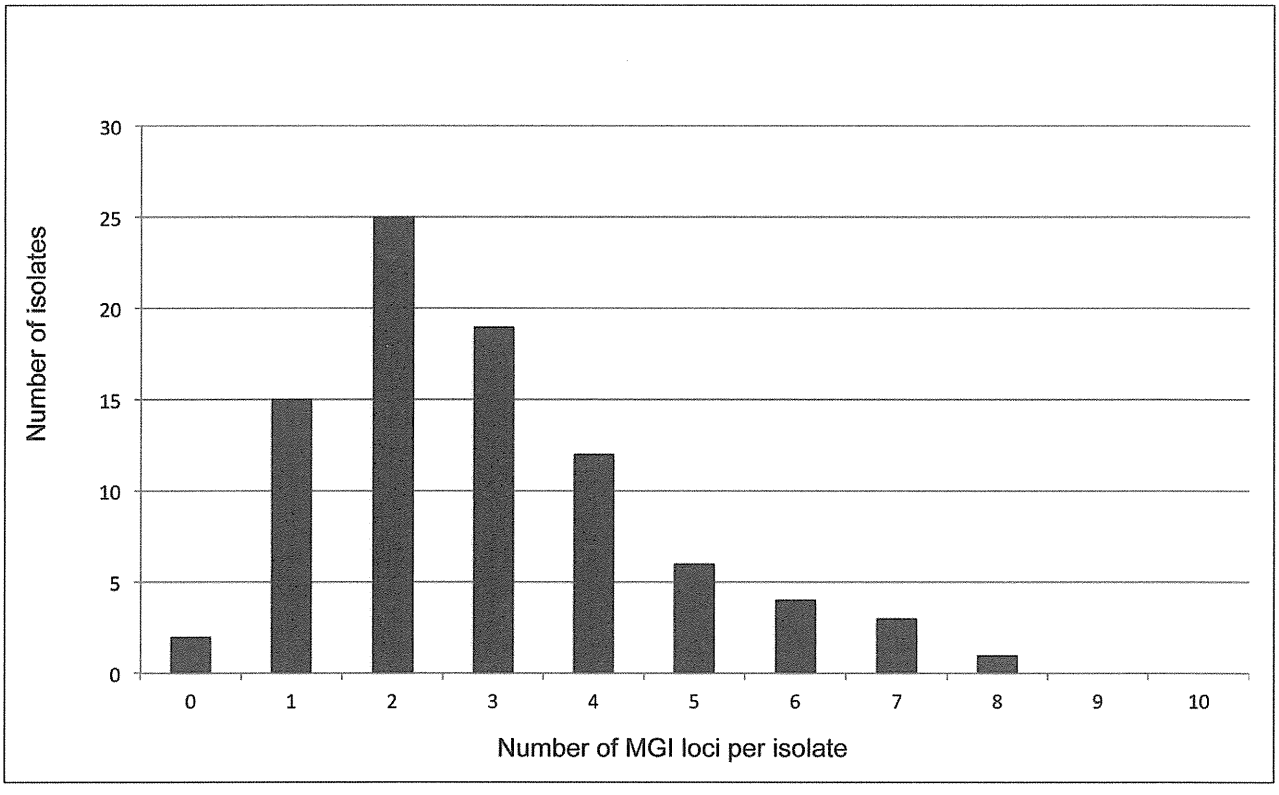


**Figure 2. Frequency of MGI loci per isolate.** Zero in the x-axis indicates that no MGI loci were observed in a particular isolate, that is, it represents a single clone infection isolate.
doi:10.1371/journal.pntd.0001592.g002

**Table 2.** Genetic diversity of *P. vivax* populations in South Korea, Sri Lanka and the Brazilian Amazon.

| Locus | Chr | Core repeat sequence in the | Type of region | South Korea (n = 87) | | Sri Lanka (n = 25) | | Brazil (n = 99) | |
|---|---|---|---|---|---|---|---|---|---|
| | (ID) | Salvador-I strain | | *A* | $H_E$ | A | $H_E$ | A | $H_E$ |
| MS1 | 3 (CM000444) | $(GAA)_{11}$ | Repeat region | 5 | 0.61 | 7 | 0.77 | 5 | 0.69 |
| MS4 | 6 (CM000447) | $(AGT)_{18}$ | Gene coding a hypothetical protein | 3 | 0.55 | 6 | 0.75 | 6 | 0.69 |
| MS5 | 6 (CM000447) | $CCTCTT(CCT)_{11}$ | Gene coding a hypothetical protein | 6 | 0.62 | 6 | 0.81 | 16 | 0.87 |
| MS6 | 11 (CM000452) | $(TCC)_2(TCT)_3(CCT)_2(TCC)_2$ $GCTTCT(TCC)_{10}$ | Repeat region | 7 | 0.66 | 6 | 0.83 | 8 | 0.66 |
| MS7 | 12 (CM000453) | $(GAA)_9$ | Between two genes* | 6 | 0.58 | 6 | 0.65 | 3 | 0.48 |
| MS8 | 12 (CM000453) | $(CAG)_2(CAA)_{11}$ | Gene coding a 3′-5′ exonuclease domein containing protein | 3 | 0.05 | 11 | 0.84 | 16 | 0.84 |
| MS9 | 8 (CM000449) | $(GGA)_{18}$ | Gene coding a hypothetical protein | 3 | 0.57 | 6 | 0.80 | 7 | 0.78 |
| MS12 | 5 (CM000446) | $(TTC)_{10}(TGC)_4$ | Repeat region | 3 | 0.07 | 6 | 0.81 | 8 | 0.74 |
| MS15 | 5 (CM000446) | $(TCT)_{10}$ | Gene coding a CW-type zinc finger domain containing protein | 5 | 0.54 | 8 | 0.86 | 16 | 0.74 |
| MS20 | 10 (CM000451) | $(GAA)_{11}GAG(GAA)_{13}(CAA)_4GAA(CAA)_5$ | Gene coding a tryptophan-rich antigen | 2 | 0.12 | 13 | 0.91 | 11 | 0.82 |
| Average | | | | 4.3 | 0.43 | 7.5 | 0.80 | 9.6 | 0.73 |

Chr: Chromosome No, ID represents Chromosome ID of *P. vivax* Salvador 1 in the GenBank Database, A: Number of alleles, *HE*: Expected heterozygosity, Data of Sri Lankan and Brazilian populations were obtained from Karunaweera, et al. (2007) [28] and Orjuela-Sánchez, et al. (2009) [33], respectively. n: Number of isolates.

*Two genes are encoding a hypothetical protein and a merozite surface protein-7.

doi:10.1371/journal.pntd.0001592.t002

2008) groups were 0.584, 0.315 and 0.140, respectively, whereas when the unique haplotypes were used in the analysis, those of the first, the second and the third were 0.408, 0.231 and 0.153, respectively (Table 4). Significant linkage disequilibrium was observed in both populations ($P<0.001$).

### Haplotypes and the relationships among the haplotypes

Microsatellite haplotypes of the 87 isolates were determined based on a combination of the allelic data of the 10 microsatellite loci; 40 haplotypes (H1–H40) were observed (Table 5). There were 2 major haplotypes (H16 and H25): H16 was observed in 9 isolates (10%) out of the 87 isolates in samples collected from 1996 to 2005; H25 was observed in 27 isolates (31%) out of the 87 isolates in samples collected from 1995 to 2003. H16 and H25 share only 3 alleles in the loci, MS8, MS12 and MS20, but those in 7 other loci were different from each other.

The relationships among the 40 haplotypes were estimated by eBURST analysis [32] with the following criterion: when 2 isolates shared more than 7 identical loci out of the 10 loci, they were connected with a branch (Fig. 4). Again, two major groups were found: Group 1 was composed of 36 isolates (41%) including the isolates with H25; Group 2 was composed of 20 isolates (23%) including those with H16. Some new or isolated haplotypes, namely H5, H6, H7, H8, H11, H12, H19, H31, H32, H33, H35, H36, that were not included in the 2 major groups or connected to any other haplotypes, have also been observed since 1998. H6 and H7 were not shown in Figure 2 because these haplotypes were quite different from the other haplotypes.

## Discussion

This is the first 15-year-long longitudinal study on *P. vivax* population genetics using highly polymorphic neutral markers. The present study demonstrated that the level of genetic diversity of the *P. vivax* population in South Korea was remarkably lower than the levels in tropical and subtropical areas reported by Karunaweera et al. [28] and Orjuela-Sánchez et al. [33] (Table 2). The 10 microsatellite loci used in the present study were a subset of the 14 loci used in the previous studies by other groups [28,33]. Imwong et al. also reported that the mean values of $H_E$ of *P. vivax* populations from Thailand (n = 28), India (n = 27) and Colombia (n = 27) were 0.77, 0.76 and 0.64, respectively [11], using 11 other microsatellite loci in the genome. These values reported by Imwong et al. were also higher than those in South Korea.

Sample size (n) and sampling conditions such as the size of sampling area and the length of sampling period may affect levels of genetic diversity of living organisms. In comparison to other studies the sample size of the present study (n = 87) was relatively large and the sampling period (15 years: from 1994 to 2008) was relatively long [11,28,33]. Generally, one would expect to see an increase in the level of genetic diversity when these conditions (a large number of samples and a long sampling period) are present. However, the South Korean *P. vivax* population showed low levels of genetic diversity, suggesting that the effective size of the re-emerged *P. vivax* population in South Korea might be small.

Microsatellite variation is strongly dependent on the length of repeat arrays [34]. Studies of numerous organisms have shown higher levels of variation in loci with long repeat arrays than those with short repeat arrays [35]. In the present study, however, even the locus with a long repeat array (MS20) showed low levels of variation in the South Korean population. Also in the same population, MS8 and MS12 showed low levels of variation, although the loci were not short repeat arrays. The genetic diversities of the loci from Sri Lankan and Brazilian populations

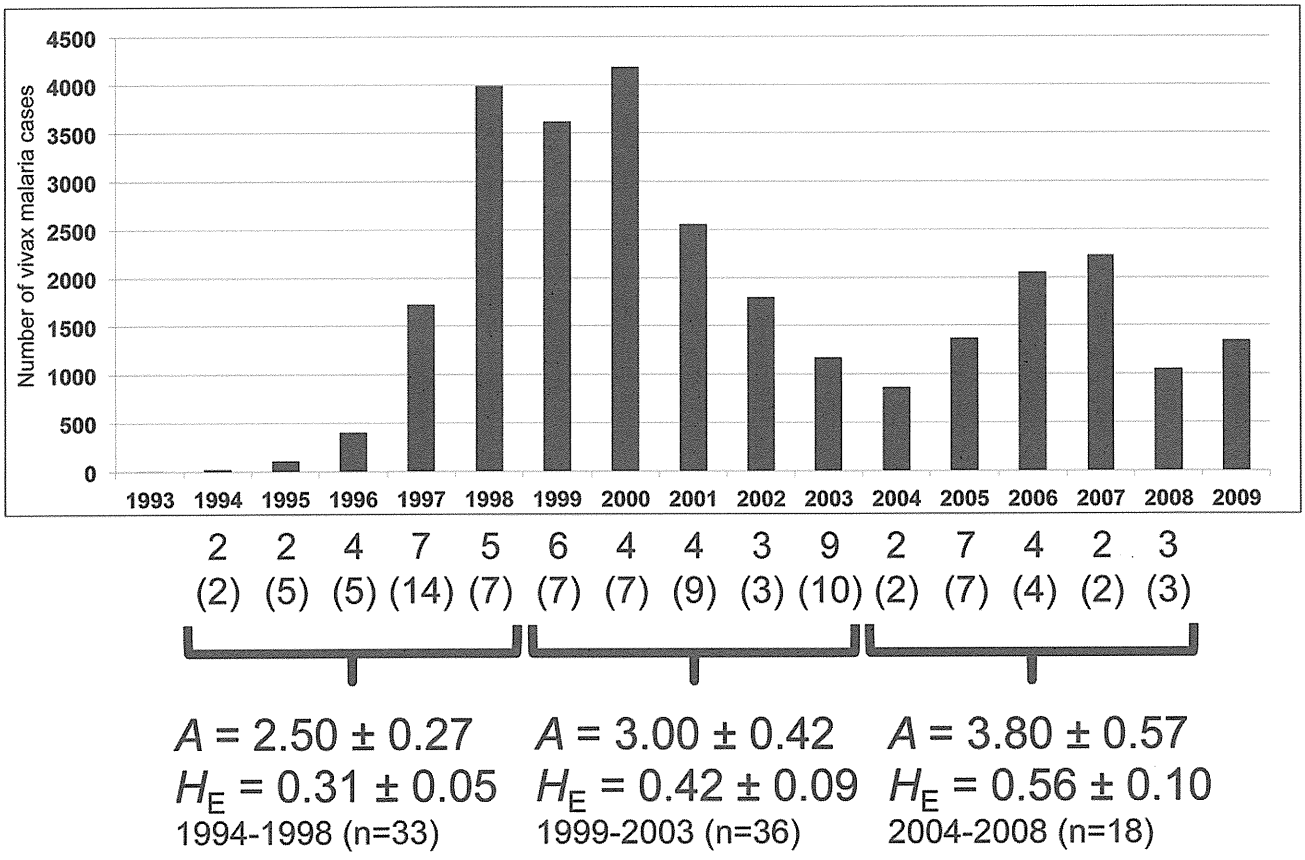


**Figure 3. Genetic diversity of the *P. vivax* population in South Korea.** *A*: Average number of the alleles ± SE, $H_E$: Average expected heterozygosity ± SE. Numbers and numbers in parentheses represent the number of haplotypes and isolates observed each year, respectively. The graph was made based on numbers of reported vivax malaria cases in South Korea. n: represents the number of isolates. The data were obtained from the *World Malaria Report 2010* (WHO) [1].
doi:10.1371/journal.pntd.0001592.g003

(Table 2) were higher than those from the South Korean population. Therefore, the uniqueness of the diversity would not be solely dependent on the characteristics of the loci. In fact, mutations of microsatellite loci are generally considered to be neutral. However, if the loci are in a certain gene or close to a certain gene, the mutation may not be strictly neutral. Indeed, 6 of the 10 loci examined in this study (MS4, MS5, MS8, MS9, MS15, MS20) were in a gene coding a hypothetical protein or a known protein (Table 2). One of the 10 loci (MS7) was between a gene coding a hypothetical protein and a gene coding a merozoite surface protein-7 which is expected to be under strong selective pressure. Therefore, the mutation of those 7 loci may not be strictly neutral. The allelic data suggested that the frequencies of strand-slippage events of the microsatellite loci during mitotic replication in the South Korean *P. vivax* population were very low because identical alleles in the known loci have been found for 10 years or longer in this population.

Multiple genotype infection (MGI) is one of the important indexes of population genetics and epidemiology of malaria parasites because MGI is the first step in recombination of the parasite genome between different clones. In the case of *P.*

**Table 3.** Multilocus linkage disequilibrium in the two *P. vivax* populations.

| Population | Single Clones | | Unique Haplotypes Only | |
|---|---|---|---|---|
| | No. | $I_A^S$ | No. | $I_A^S$ |
| 1994–2000 | 47 | 0.529*** | 19 | 0.346*** |
| 2001–2008 | 40 | 0.218*** | 27 | 0.173*** |

Single clones show all haplotypes in single-clone infections. Unique haplotypes show haplotypes excluding duplicates of any multiply represented infection. No. indicates the number of isolates for each measure.
***$P<0.001$.
doi:10.1371/journal.pntd.0001592.t003

**Table 4.** Multilocus linkage disequilibrium in the two *P. vivax* populations.

| Population | Single Clones | | Unique Haplotypes Only | |
|---|---|---|---|---|
| | No. | $I_A^S$ | No. | $I_A^S$ |
| 1994–1998 | 33 | 0.584*** | 13 | 0.408*** |
| 1999–2003 | 36 | 0.315*** | 17 | 0.231*** |
| 2004–2008 | 18 | 0.140*** | 18 | 0.153*** |

Single clones show all haplotypes in single-clone infections. Unique haplotypes show haplotypes excluding duplicates of any multiply represented infection. No. indicates the number of isolates for each measure.
***$P<0.001$.
doi:10.1371/journal.pntd.0001592.t004

**Table 5.** Forty haplotypes of the *P. vivax* population in South Korea based on 10 microsatellite DNA loci.

| H | Year | | | | | | | | | | | | | | | Total |
|---|---|---|---|---|---|---|---|---|---|---|---|---|---|---|---|---|
| | 1994 | 1995 | 1996 | 1997 | 1998 | 1999 | 2000 | 2001 | 2002 | 2003 | 2004 | 2005 | 2006 | 2007 | 2008 | |
| H1 | | | | | | | | | | | | *1* | | | | *1* |
| H2 | *1* | | | | | | | | | | | | | | | *1* |
| H3 | | | | | | | *1* | | | | | | | | | *1* |
| H4 | | | *1* | | | | | | | | | | | | | *1* |
| H5 | | | | | | | | | | | | *1* | | | | *1* |
| H6 | | | | | | | | | | | | | *1* | | | *1* |
| H7 | | | | | | | | | | | | | | | *1* | *1* |
| H8 | | | | | | | | | | | *1* | | | | | *1* |
| H9 | | | | | | | | | | *1* | | *1* | | | | *2* |
| H10 | | | | | | | | | | *1* | | | *1* | | | *2* |
| H11 | | | | | | | | | | | | | | *1* | | *1* |
| H12 | | | | | | | | | | *1* | | | | | | *1* |
| H13 | | | | *1* | | | | | | | | | | | | *1* |
| H14 | | | | *1* | | | | *1* | | | | | | | | *2* |
| H15 | | | | | | | *1* | | | | | | | | | *1* |
| **H16** | | | **1** | | **1** | **2** | **2** | **2** | | | | **1** | | | | **9** |
| H17 | | | | *1* | | | | | | | | | | | | *1* |
| H18 | | | | | | *1* | | | *1* | | | | | | | *2* |
| H19 | | | | | | | | | | | | | | | *1* | *1* |
| H20 | *1* | | | | | | | | | | *1* | | | | | *2* |
| H21 | | | *1* | | | | | | | | | | | | | *1* |
| H22 | | | | | *1* | | | | | | | | | | | *1* |
| H23 | | | | | | | | | | *1* | | | | | | *1* |
| H24 | | *1* | | *1* | *1* | | | | | | | | | | | *3* |
| **H25** | | **4** | **2** | **8** | **3** | **1** | **3** | **4** | | **2** | | | | | | **27** |
| H26 | | | | *1* | | | | | | | | *1* | | | | *2* |
| H27 | | | | *1* | | | | | | | | | | | | *1* |
| H28 | | | | | | *1* | | | | | | | | | | *1* |
| H29 | | | | | | | | | | *1* | | | | | | *1* |
| H30 | | | | | | | | | | *1* | | | | | | *1* |
| H31 | | | | | | | | | | | | | | *1* | | *1* |
| H32 | | | | | | | | | | | | *1* | | | | *1* |
| H33 | | | | | *1* | | | *2* | *1* | | | | | | | *4* |
| H34 | | | | | | *1* | | | | | | | | | | *1* |
| H35 | | | | | | *1* | | | | | | | | | | *1* |
| H36 | | | | | | | | | | | | | *1* | | | *1* |
| H37 | | | | | | | | | | *1* | | | | | | *1* |
| H38 | | | | | | | | | *1* | *1* | | | *1* | | | *3* |
| H39 | | | | | | | | | | | | *1* | | | | *1* |
| H40 | | | | | | | | | | | | | | | *1* | *1* |
| Total | 2 | 5 | 5 | 14 | 7 | 7 | 7 | 9 | 3 | 10 | 2 | 7 | 4 | 2 | 3 | 87 |

H: Haplotype, Numbers show number of isolates. Total: Total No. of isolates, Two predominant haplotypes, and H25 are highlighted in bold and the other haplotypes are highlighted in italic.

doi:10.1371/journal.pntd.0001592.t005

*falciparum*, the rate of MGIs per population is basically associated with the endemicity [4,5]. That is, the MGI rate of *P. falciparum* population is higher in high transmission areas and lower in low transmission areas. However, this is not the case with *P. vivax* populations because high MGI rates were observed among the *P. vivax* populations in low transmission areas [11,12]. This feature could be attributed to relapse owing to hypnozoites in the liver of a vivax malaria patient. Although MGI is an important index, the methods or criteria of determining MGI is problematic. When any locus of the 10 loci showed more than 1 allele, we regarded the

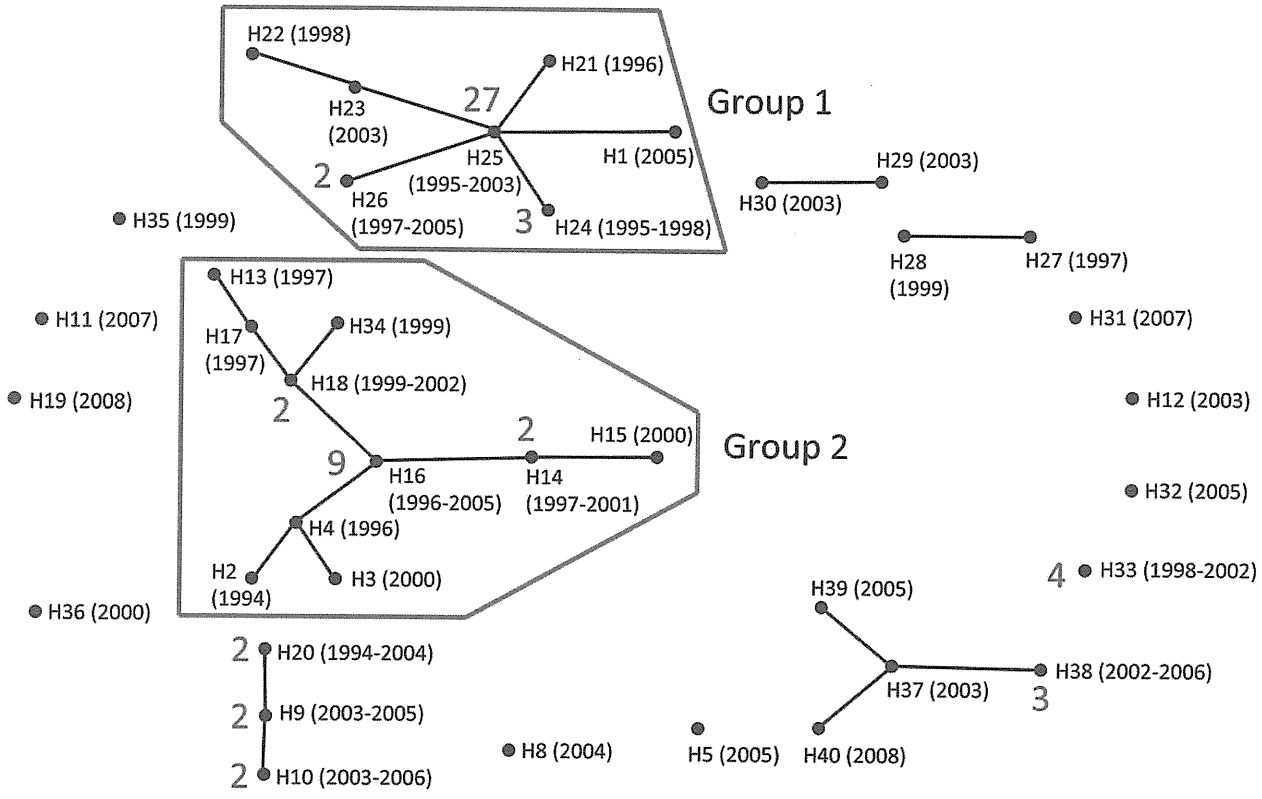


**Figure 4. Relationships among the 40 haplotypes of *P. vivax* (n = 87) in South Korea estimated by eBURST analysis.** Relationships among 40 microsatellite haplotypes in the 87 isolates collected in South Korea as defined by eBURST analysis [32]. H1, H2, ... H40 represent the microsatellite haplotype. Red numbers represent the number of isolates that showed the haplotype. When the haplotype was found in only one isolate, the red number was omitted. Numbers in parentheses represent the year the haplotype was observed. H6 and H7 were included in the analysis but were classified into a different group because they were considerably different from others and were omitted from Figure 4.
doi:10.1371/journal.pntd.0001592.g004

isolate as an example of MGI. Using this method, 85 (97.7%) out of the 87 isolates were MGIs. Focusing on each locus, the MGI rate per locus varied from 0.0% to 83.9% (average 29.1%) (Table 1). Focusing on the number of MGI loci per isolate, we found an interesting distribution pattern, similar to an F-distribution (Fig. 2). In the present study, the highest frequency of MGI loci per isolate was 2 (found in 25 isolates). The frequency decreased gradually, that is, 3 MGI loci; 19 isolates, 4 MGI loci; 12 isolates, 5 MGI loci; 6 isolates, and so on. We suspect that this distribution pattern may vary in each endemic area with different endemicity.

In the case of *P. falciparum* populations, the levels of genetic diversity are normally associated with the levels of malaria endemicity. That is, the levels of genetic diversity of the parasite populations are higher in high transmission areas and lower in low transmission areas [4,5], although some exceptions have been reported [36].

We suspect that there will also be some association between the levels of genetic diversity and the levels of malaria endemicity in *P. vivax* populations, even though the correlation between these factors is not clearly understood at the time of writing. In *P. vivax* populations, the levels of genetic diversity tend to be high even in low transmission areas [11–13,28]. This tendency can likely be attributed to unique biological features of *P. vivax*, such as early gametocytogenesis and relapse. Early gametocytogenesis may enhance the efficiency of transmission to *Anopheles* mosquitoes, allowing transmission to occur before symptoms appear – or, more importantly, before antimalarial drugs are administered. Relapses may also enhance the transmission and increase the genetic diversity of *P. vivax* populations, because the relapse will increase the probability of the coexistence of multiple genotype clones in a single patient, which are subsequently sucked up by an *Anopheles* mosquito in a single meal. Thus, the levels of genetic diversity of *P. vivax* populations could be higher than those observed in *P. falciparum* populations even in low transmission areas.

In the present study, the levels of genetic diversity of the South Korean population between 1994 and 2000 (when the number of malaria cases increased) were relatively lower than the levels of genetic diversity between 2001 and 2008 (when the number decreased). On the contrary, the levels of multilocus LD in the population between 1994 and 2000 were relatively higher than those between 2001 and 2008. These results suggested that the latter population was more genetically diverse and had less inbreeding. Furthermore, we divided the population into 3 groups each covering 5-year periods (1994–1998, 1999–2003 and 2004–2008) and reexamined the levels of genetic diversity and multilocus LD. Then, we again observed that the levels of genetic diversity in the populations had gradually increased, whereas the levels of multilocus LD had gradually decreased even though there was still strong multilocus LD in the most recent population (2004–2008). This result was surprising to us because we expected that the effective population size of the latter population would have decreased due to the reduction in the number of alleles in the population. However, this was not the case. In the South Korean populations, the association between the diversity and the endemicity of the *P. vivax* population is elusive.

There are, however, at least two possible explanations for this result. One is that the levels of genetic diversity of the *P. vivax* population increased in North Korea from 2001 to 2002, while the number of vivax malaria cases was very high (296,540 cases in 2001, 241,190 cases in 2002) [1]. Some of the isolates might have then been introduced to South Korea from North Korea by *Anopheles* mosquitoes. The other possible explanation is that the genetic diversity began accumulating in the South Korean population after the re-emergence in 1993. If the latter hypothesis is correct then the malaria control program conducted by the South Korean government might not have affected the parasite population structure.

One of the clear differences between the *P. vivax* population in South Korea and populations in tropical and subtropical areas is the pattern of transmission: in South Korea, vivax malaria is seasonally prevalent with a peak during July and August and no transmission in the winter season [37] and very long incubation periods with 8 to 13 months [14], suggesting that the chance for the recombination of the genome is limited to specific time periods within the year, possibly once or at most twice a year. In fact, we found strong LD in the South Korean population, suggesting that the frequency of recombination in this population would be very limited. However, these results might be associated with the location of the examined MS DNA loci: the 6 loci are in a gene coding a protein and another locus is between 2 genes coding respective proteins. In tropical and subtropical areas, on the other hand, vivax malaria is prevalent throughout the year, and thus recombination may occur throughout the year; this would lead to an increase in the levels of genetic diversity in tropical and subtropical areas. Indeed, in the populations from the Brazilian Amazon, identical haplotypes were rarely observed two years in a row, even in the same endemic area [12]. This would suggest that frequent recombinations occurred between the clones in the population.

The present study showed evidence of a low recombination rate and low frequencies of strand-slippage events of the microsatellite loci during mitotic replication in the *P. vivax* population of South Korea in comparison to populations in tropical and subtropical areas [12], and demonstrated that the 2 dominant haplotypes (H16 and H25) had been transmitting for several years (H16; 1996, 1998–2001, 2005, H25; 1995–2001, 2003) (Table 5). This continuous existence of the same haplotypes for several years is definitive evidence of a low recombination rate in the South Korean *P. vivax* population.

This continuous existence of the same haplotypes could be explained by a local adaptation to vector species. According to Joy et al. [38], for example, *P. vivax* in southern Mexico was genetically differentiated into 3 populations. They suggested that this differentiation would be the result of adaptation to different *Anopheles* species. On the other hand, in South Korea, *Anopheles sinensis* is a main vector of *P. vivax* and the other *Anopheles* species are very minor. Therefore, continuous existence of the predominant haplotypes could not be explained by a local adaptation to certain vector species in this country. There might be some other advantages of these haplotypes, or simply, the variation in the *P. vivax* population on the Korean peninsula had been very small owing to an effective national eradication program conducted by the National Malaria Eradication Service under the operation of the South Korean government with the support of the WHO in the 1970s [14–16].

Although the predominant haplotypes (H16 and H25) and their relatives had been transmitting in the DMZ for a long time, their transmission ended in 2005. We speculate that these predominant haplotypes were probably eliminated by the malaria control programs conducted by the North Korean government. In fact, according to the WHO World Malaria Report 2010, the number of vivax malaria cases in North Korea decreased substantially (2001: 296540 cases, 2005: 11507 cases). The reason for this reduction was not mentioned in detail, however this is probably due to the effect of mass drug administration by the North Korean government supported by South Korea. We suspect that the population structure of *P. vivax* in North Korea was changed dramatically and that these predominant "old" haplotypes were eliminated completely or became very minor in both the North Korean and South Korean populations. We suspect that the South Korean *P. vivax* population is a subpopulation of the North.

Our previous genetic epidemiological analyses of the South Korean *P. vivax* population using antigenic molecules [21–25] and the mitochondrial genome [39] showed that there were 2 types (or groups) of parasite populations in the endemic area. In these previous studies we examined groups of isolates collected from vivax malaria patients in the DMZ in 1997 [21], 1998 [22–24], 1999 [39]. In the present study, we examined isolates collected from patients in the DMZ between 1994 and 2008 using 10 highly polymorphic microsatellite loci. Once again, we observed two types of parasite populations (Fig. 4). However, some other haplotypes (clones) have been observed in the endemic area since 1998. The new haplotypes were genetically different to the 2 major groups that have been transmitted since the beginning of the re-emergence (Fig. 4). This finding was consistent with the results of analyses by Choi et al. using the DNA sequences of 2 antigenic molecules (circumsporozoite protein, merozoite surface protein-1) of isolates collected in the DMZ from 1996 to 2007 [40]. They also reported that new genotypes have been observed since 2000 and that the new genotypes had been rapidly disseminated in the endemic area.

The genetic differences between the 2 major groups and the new haplotypes in our data suggested two possibilities: the new haplotypes could have arisen in the DMZ in South Korea through recombination between existing clones in the population; or their emergence could be attributed to a continual introduction of *P. vivax* from other population sources, probably from North Korea. The present study suggested a low recombination rate in the South Korean population and would seem to indicate that the latter possibility is more likely.

A less likely possibility is that all of the isolates examined in this study were continually introduced from North Korea because all the isolates were collected from South Korean soldiers who served in the DMZ. These patients were normally treated by chloroquine within 4 days of the onset of the symptoms, and then treated by primaquine as a radical cure. The recurrence rate (both new infection and relapse may be included) of vivax malaria among them is 1.6% (62 cases of 3881 cases) and the definitive relapse rate is only 0.2% (8 cases of 3881 cases) [41]. In addition, the incubation period of *P. vivax* on the Korean peninsula is very long (8 months to 13 months) [14] and the transmission is mainly in summer [38]. Moreover, the period of conscription is about 2 years. Therefore, it might have been very difficult to transmit continuously among the South Korean soldiers in the DMZ, leading to the high recombination rate of the genome within the parasite population of the study area.

There are a number of sampling limitations to the present study. The number of isolates per year was relatively small (2 to 14 isolates, average: 5.8 isolates/year), and the sample size during the years 2004–2008 was particularly small (2 to 7 isolates, average: 3.6 isolates/year). Moreover, all of the isolates used in this study were collected only from South Korean soldiers or veterans and not from civilians, whose proportion among vivax malaria patients in South Korea has been gradually increasing [18]. In order to

overcome these limitations and more accurately estimate the current status of the parasite population in South Korea, it will be necessary to include new isolates collected from civilians in the endemic areas and to increase the sample size of recent years.

Although travel between South and North Korea is basically restricted and the malaria control programs in the two countries may not be the same, we suspect that the South Korean *P. vivax* population is a subpopulation of the North Korean population because the majority of malaria patients live near the border [42]. *Anopheles* mosquitoes can fly over the DMZ, and South Korean travelers are allowed to visit some parts of North Korea, such as Kaesong and Kumgang-san, which are very famous for sightseeing. Furthermore, from 2001 to 2009 the number of vivax malaria cases in North Korea ranged from twice as high as the number in South Korea to many times higher, indicating that the size of the parasite population in North Korea is probably larger. Thus, the inclusion of North Korean isolates in the analyses would greatly enhance the accuracy of the estimation of the parasite population structure and the transmission dynamics and provide a more complete picture of the *P. vivax* population in the Korean peninsula; unfortunately the feasibility of doing this is low.

In conclusion, molecular epidemiology using highly polymorphic DNA markers of the *P. vivax* population is a very useful tool for assessing the population structure and transmission dynamics of the parasites, the knowledge of which may lead to the effective control of vivax malaria in the respective endemic areas.

## Author Contributions

Conceived and designed the experiments: MI MF WGK SK. Performed the experiments: MI MF SYH SHK. Analyzed the data: MI MF. Contributed reagents/materials/analysis tools: WGK. Wrote the paper: MI MF WGK SK.

## References


1. World Health Organization (2010) World Malaria Report 2010. Geneva: WHO.
2. Guerra CA, Howes RE, Patil AP, Gething PW, Van Boeckel TP, et al. (2010) The international limits and population at risk of *Plasmodium vivax* transmission in 2009. PLoS Negl Trop Dis 4: e774.
3. Enserink M (2010) As challenges change, so does science. Science 328: 843.
4. Iwagami M, Rivera PT, Villacorte EA, Escueta AD, Hatabu T, et al. (2009) Genetic diversity and population structure of *Plasmodium falciparum* in the Philippines. Malar J 8: 96.
5. Anderson TJ, Haubold B, Williams JT, Estrada-Franco JG, Richardson L, et al. (2000) Microsatellite markers reveal a spectrum of population structures in the malaria parasite *Plasmodium falciparum*. Mol Biol Evol 17: 1467–1482.
6. Machado RL, Povoa MM, Calvosa VS, Ferreira MU, Rossit AR, et al. (2004) Genetic structure of *Plasmodium falciparum* populations in the Brazilian Amazon region. J Infect Dis 190: 1547–1555.
7. Anthony TG, Conway DJ, Cox-Singh J, Matusop A, Ratnam S, et al. (2005) Fragmented population structure of *Plasmodium falciparum* in a region of declining endemicity. J Infect Dis 191: 1558–1564.
8. Mu J, Joy DA, Duan J, Huang Y, Carlton J, et al. (2005) Host switch leads to emergence of *Plasmodium vivax* malaria in humans. Mol Biol Evol 22: 1686–1693.
9. Jongwutiwes S, Putaporntip C, Iwasaki T, Ferreira MU, Kanbara H, et al. (2005) Mitochondrial genome sequences support ancient population expansion in *Plasmodium vivax*. Mol Biol Evol 22: 1733–1739.
10. Cornejo OE, Escalante AA (2006) The origin and age of *Plasmodium vivax*. Trends Parasitol 22: 558–563.
11. Imwong M, Nair S, Pukrittayakamee S, Sudimack D, Williams JT, et al. (2007) Contrasting genetic structure in *Plasmodium vivax* populations from Asia and South America. Int J Parasitol 37: 1013–1022.
12. Ferreira MU, Karunaweera ND, da Silva-Nunes M, da Silva NS, Wirth DF, et al. (2007) Population structure and transmission dynamics of *Plasmodium vivax* in rural Amazonia. J Infect Dis 195: 1218–1226.
13. Gunawardena S, Karunaweera ND, Ferreira MU, Phone-Kyaw M, Pollack RJ, et al. (2010) Geographic structure of *Plasmodium vivax*: microsatellite analysis of parasite populations from Sri Lanka, Myanmar, and Ethiopia. Am J Trop Med Hyg 82: 235–242.
14. Chai JY (1999) Re-emerging *Plasmodium vivax* malaria in the Republic of Korea. Korean J Parasitol 37: 129–143.
15. Ree HI (2000) Unstable vivax malaria in Korea. Korean J Parasitol 38: 119–138.
16. Shin EH, Guk SM, Kim HJ, Lee SH, Chai JY (2008) Trends in parasitic diseases in the Republic of Korea. Trends Parasitol 24: 143–150.
17. Chai IH, Lim GI, Yoon SN, Oh WI, Kim SJ, et al. (1994) [Occurrence of tertian malaria in a male patient who has never been abroad]. Korean J Parasitol 32: 195–200 [Article in Korean, English abstract available].
18. Park JW, Jun G, Yeom JS (2009) *Plasmodium vivax* malaria: status in the Republic of Korea following reemergence. Korean J Parasitol 47(Suppl): S39–50.
19. Han ET, Lee DH, Park KD, Seok WS, Kim YS, et al. (2006) Reemerging vivax malaria: changing patterns of annual incidence and control programs in the Republic of Korea. Korean J Parasitol 44: 285–294.
20. Feighner BH, Pak SI, Novakoski WL, Kelsey LL, Strickman D (1998) Reemergence of *Plasmodium vivax* malaria in the Republic of Korea. Emerg Infect Dis 4: 295–297.
21. Kho WG, Park YH, Chung JY, Kim JP, Hong ST, et al. (1999) Two new genotypes of *Plasmodium vivax* circumsporozoite protein found in the Republic of Korea. Korean J Parasitol 37: 265–270.
22. Kho WG, Chung JY, Sim EJ, Kim DW, Chung WC (2001) Analysis of polymorphic regions of *Plasmodium vivax* Duffy binding protein of Korean isolates. Korean J Parasitol 39: 143–150.
23. Chung JY, Chun EH, Chun JH, Kho WG (2003) Analysis of the *Plasmodium vivax* apical membrane antigen-1 gene from re-emerging Korean isolates. Parasitol Res 90: 325–329.
24. Kim SH, Hwang SY, Shin JH, Moon CS, Kim DW, et al. (2009) Molecular genetic characterization of the merozoite surface protein 1 Gene of *Plasmodium vivax* from reemerging Korean isolates. Clin Vaccine Immunol 16: 733–738.
25. Hwang SY, Kim SH, Kho WG (2009) Genetic characteristics of polymorphic antigenic markers among Korean isolates of *Plasmodium vivax*. Korean J Parasitol 47(Suppl): S51–58.
26. Hartl DL (2004) The origin of malaria: mixed messages from genetic diversity. Nat Rev Microbiol 2: 15–22.
27. Sambrook J, Russell DW (2001) Molecular Cloning: A Laboratory Manual. 3rd edition. New York: Cold Spring Harbor Laboratory Press. pp 6.4–6.12.
28. Karunaweera ND, Ferreira MU, Hartl DL, Wirth DF (2007) Fourteen polymorphic microsatellite DNA markers for the human malaria parasite *Plasmodium vivax*. Mol Ecol Notes 7: 172–175.
29. Maynard-Smith J, Smith NH, O'Rourke M, Spratt BG (1993) How clonal are bacteria? Proc Natl Acad Sci USA 90: 4384–4388.
30. Hudson RR (1994) Analytical results concerning linkage disequilibrium in models with genetic transformation and recombination. J Evol Biol 7: 535–548.
31. Haubold B, Hudson RR (2000) LIAN 3.0: detecting linkage disequilibrium in multilocus data. Linkage Analysis. Bioinformatics 16: 847–848.
32. Feil EJ, Li BC, Aanensen DM, Hanage WP, Spratt BG (2004) eBURST: inferring patterns of evolutionary descent among clusters of related bacterial genotypes from multilocus sequence typing data. J Bacteriol 186: 1518–30.
33. Orjuela-Sánchez P, da Silva NS, da Silva-Nunes M, Ferreira MU (2009) Recurrent parasitemias and population dynamics of *Plasmodium vivax* polymorphisms in rural Amazonia. Am J Trop Med Hyg 81: 961–968.
34. Imwong M, Sudimack D, Pukrittayakamee S, Osorio L, Day NPJ, et al. (2006) Microsatellite variation, repeat array length and population history of *Plasmodium vivax*. Mol Biol Evol 23: 1016–1018.
35. Ellegren H (2004) Microsatellites: simple sequences with complex evolution. Nat Rev Genet 5: 435–445.
36. Branch OH, Sutton PL, Castro JC, Barnes C, Hussin J, et al. (2011) *Plasmodium falciparum* genetic diversity maintained and amplified over 5 years of a low transmission endemic in the Peruvian Amazon. Mol Biol Evol 28: 1973–1986.
37. Park JW, Klein TA, Lee HC, Pacha LA, Ryu SH, et al. (2003) Vivax malaria: a continuing health threat to the Republic of Korea. Am J Trop Med Hyg 69: 159–167.
38. Joy DA, Gonzalez-Ceron L, Carlton JM, Gueye A, Fay M, et al. (2008) Local adaptation and vector-mediated population structure in *Plasmodium vivax* malaria. Mol Biol Evol 25: 1245–1252.
39. Iwagami M, Hwang SY, Fukumoto M, Hayakawa T, Tanabe K, et al. (2010) Geographical origin of *Plasmodium vivax* in the Republic of Korea: haplotype network analysis based on the parasite's mitochondrial genome. Malar J 9: 184.
40. Choi YK, Choi KM, Park MH, Lee EG, Kim YJ, et al. (2010) Rapid dissemination of newly introduced *Plasmodium vivax* genotypes in South Korea. Am J Trop Med Hyg 82: 426–432.
41. Moon KT, Kim YK, Ko DH, Park I, Shin DC, et al. (2009) Recurrence rate of vivax malaria in the Republic of Korea. Trans R Soc Trop Med Hyg 103: 1245–1249.
42. Roll Back Malaria, World Health Organization, UNICEF (2005) Democratic People's Republic of Korea, Country Profile, World Malaria Report 2005. Geneva: WHO and UNICEFAvailable: http://www.rollbackmalaria.org/wmr2005/profiles/dprkorea.pdf. Accessed: 2011 Sep 14.

Vaccine 30 (2012) 1807–1812

Contents lists available at SciVerse ScienceDirect

Vaccine

journal homepage: www.elsevier.com/locate/vaccine

# *Plasmodium vivax* gametocyte protein Pvs230 is a transmission-blocking vaccine candidate

Mayumi Tachibana[a], Chiho Sato[a], Hitoshi Otsuki[b], Jetsumon Sattabongkot[c,1], Osamu Kaneko[d], Motomi Torii[a,e,**], Takafumi Tsuboi[e,f,g,*]

[a] *Department of Molecular Parasitology, Ehime University Graduate School of Medicine, Shitsukawa, Toon, Ehime 791-0295, Japan*
[b] *Division of Medical Zoology, Faculty of Medicine, Tottori University, Yonago, Tottori 683-8503, Japan*
[c] *Department of Entomology, Armed Forces Research Institute of Medical Sciences, Bangkok 10400, Thailand*
[d] *Department of Protozoology, Institute of Tropical Medicine (NEKKEN) and the Global Center of Excellence Program, Nagasaki University, Sakamoto, Nagasaki 852-8523, Japan*
[e] *Ehime Proteo-Medicine Research Center, Ehime University, Toon, Ehime 791-0295, Japan*
[f] *Cell-Free Science and Technology Research Center, Ehime University, Matsuyama, Ehime 790-8577, Japan*
[g] *Venture Business Laboratory, Ehime University, Matsuyama, Ehime 790-8577, Japan*

ARTICLE INFO

*Article history:*
Received 29 July 2011
Received in revised form
24 December 2011
Accepted 2 January 2012
Available online 11 January 2012

*Keywords:*
DNA vaccine
Gametocyte
Malaria
*Plasmodium vivax*
Pvs230
Transmission-blocking vaccine

ABSTRACT

The malaria transmission-blocking vaccine (TBV) aims to interfere the development of malaria parasite in the mosquito and prevent further transmission in the community. So far only two TBV candidates have been identified in *Plasmodium vivax*; ookinete surface proteins Pvs25 and Pvs28. The *pvs230* (PVX_003905) is reported as an ortholog of Pfs230, a gametocyte/gamete stage TBV candidate in *Plasmodium falciparum*, however its candidacy for TBV has never been tested. Therefore here, we have investigated whether Pvs230 can be a TBV candidate using *P. vivax* samples obtained from Thailand. The mouse antiserum raised against the plasmid expressing CRDs I–IV of Pvs230 detected Pvs230 protein in the lysate of *P. vivax* gametocyte in western blot analysis under non-reducing condition. From the localization of Pvs230 on the outer most regions of gametocyte in the immunofluorescence assay, it appears that Pvs230 is localized on the surface of gametes. Importantly, the anti-Pvs230 mouse serum significantly reduced the number of *P. vivax* oocysts developed in the mosquito midgut. Moreover, the polymorphism in Pvs230 CRDs I–IV is limited suggesting that it may not be an impediment for the utilization of Pvs230 as an effective TBV candidate. In conclusion, our results show that Pvs230 is a transmission-blocking vaccine candidate of *P. vivax*.



## 1. Introduction

Malaria is one of the major global public health problems which inhibit social and economic development of vast areas of the tropical regions of the world [1]. While malaria mortality is mainly due to the infection of *Plasmodium falciparum*, *Plasmodium vivax* remains to be a huge burden to the communities in Asia, Pacific, and Central and South America. The emergence of mosquito strains resistant to insecticides and parasites resistant to anti-malarial drugs is a major limiting factor making malaria eradication difficult [2,3]. Moreover, a recent study showed that though the incidence of *P. falciparum* could be eliminated by the malaria mass drug treatment in an island in Vanuatu, still the *P. vivax* cases remained [4]. Therefore, the development of vaccines against *P. vivax* is also an essential component towards malaria elimination [5].

At present there are only two leading vivax vaccine candidates in Phase I of the vaccine development pipeline [5]; circumsporozoite protein (CSP) (a pre-erythrocytic vaccine candidate which acts against sporozoites and liver-stage parasites and prevent infection) [6] and Pvs25 (a transmission-blocking vaccine (TBV) candidate which blocks malaria transmission by interrupting the parasite life cycle in the mosquito midgut) [7,8].

TBV targets the molecules of the sexual stage parasites in mosquito (i.e., gametocyte, gamete, zygote, and ookinete) and in human (gametocyte). The leading targets for TBV are ookinete surface proteins; Pfs25 in *P. falciparum* [9] and Pvs25 and Pvs28 in *P. vivax* [10]. Both Pfs25 and Pvs25 are expressed only on the surface

* Corresponding author at: Cell-Free Science and Technology Research Center, Ehime University, Matsuyama, Ehime 790-8577, Japan.
Tel.: +81 89 927 8277; fax: +81 89 927 9941.
** Corresponding author at: Department of Molecular Parasitology, Ehime University Graduate School of Medicine, Toon, Ehime 791-0295, Japan. Tel.: +81 89 960 5285; fax: +81 89 960 5287.
*E-mail addresses:* torii@m.ehime-u.ac.jp (M. Torii), tsuboi@ccr.ehime-u.ac.jp (T. Tsuboi).
[1] Present address: Mahidol Vivax Research Center, Faculty of Tropical Medicine, Mahidol University, Bangkok, Thailand.

0264-410X/$ – see front matter © 2012 Elsevier Ltd. All rights reserved.
doi:10.1016/j.vaccine.2012.01.003

of mosquito stage parasites (zygote and ookinete). On the other hand, Pfs230, a TBV candidate of *P. falciparum*, is expressed both in human (gametocytes) and mosquito stages (gametes) [11,12]. Pfs230 is a member of the 6-cys protein family [13], and it is predicted to have a complex tertiary structure due to the presence of fourteen cysteine-rich domains (CRDs) [14,15]. Polyclonal antibody against recombinant Pfs230 region C [amino acid positions (aa) 443–1132] expressed both in *Escherichia coli* [16] and in wheat germ cell-free system [12] exhibited transmission-blocking activity (i.e., reduced the infectivity of *P. falciparum* to mosquitoes). These evidences support the rationale to prioritize the N-terminal domain of Pfs230 as falciparum TBV candidate.

Since Pvs230 in *P. vivax* is an ortholog of Pfs230, we recently performed an evolutionary and population genetic analysis on Pvs230 gene (*pvs230*: PVX_003905) using *pvs230* nucleotide sequences of field isolates collected worldwide [17]. We found that the fourteen CRDs in Pvs230 are more conserved and less polymorphic among different *Plasmodium* species (i.e. *P. falciparum*, *P. knowlesi*, *P. cynomolgi*, *P. yoelii*, *P. berghei*, *P. chabaudi*, and *P. gallinaceum*). [17]. These results reinforce the rationale that CRDs of Pvs230 can be a target of vivax TBV. Here we report that anti-Pvs230 antibody raised by DNA immunization with a plasmid expressing CRDs I–IV of Pvs230 not only recognized the native Pvs230 protein on the western blot of *P. vivax* gametocyte lysates, but also exhibited a transmission-blocking activity on the field *P. vivax* isolates from Thailand.

## 2. Materials and methods

### 2.1. Parasite collection and DNA preparation

Genomic DNA (gDNA) was extracted as described previously [10] from Salvador 1 (Sal-1) of *P. vivax* maintained in the chimpanzee (a generous gift of Dr. William Collins, CDC, Atlanta, GA). gDNA from the following patient samples used for the membrane feeding assay were also extracted as previously described [17].

Peripheral blood was collected from volunteer *P. vivax* patients after the written informed consent in Mae Sod malaria clinic in Tak province, northwestern Thailand. A single infection of *P. vivax* was diagnosed by conventional microscopy and confirmed by nested PCR. For nested PCR, the species-specific nucleotide sequences of the 18S rRNA genes of *P. falciparum*, *P. vivax*, *P. malariae*, and *P. ovale* were amplified as described previously [18]. All research involving human subjects in this study was reviewed and approved by the Institutional Ethics Committee of the Thai Ministry of Public Health and the Human Subjects Research Review Board of the United States Army.

Firstly, the leukocytes were removed from *P. vivax* infected blood collected from Thai patients by passing the blood through CF-11 column. Secondly, the leukocyte-removed blood was subjected to Percoll density gradient centrifugation to obtain gametocyte-infected erythrocytes. The fraction containing the gametocyte-infected erythrocytes was used for immunofluorescence, and immunoblotting analyses.

### 2.2. Plasmid DNA construction, purification, and formulation with Vaxfectin®

Based on the previous findings that Pfs230C (aa 443–1132) (Fig. 1B) is a transmission blocking vaccine candidate [12,16], here we focused on characterizing the N-terminal domain of putative mature Pvs230 as a prime TBV candidate domain. DNA fragment encoding Pvs230 CRDs I–IV (aa 236–943) (Fig. 1A) was amplified from *P. vivax* Sal-1 strain gDNA with a sense primer, Pvs230-VR-F1 (5′-ggatccGTCTTCGACAAGGTGGACG-3′) and an antisense

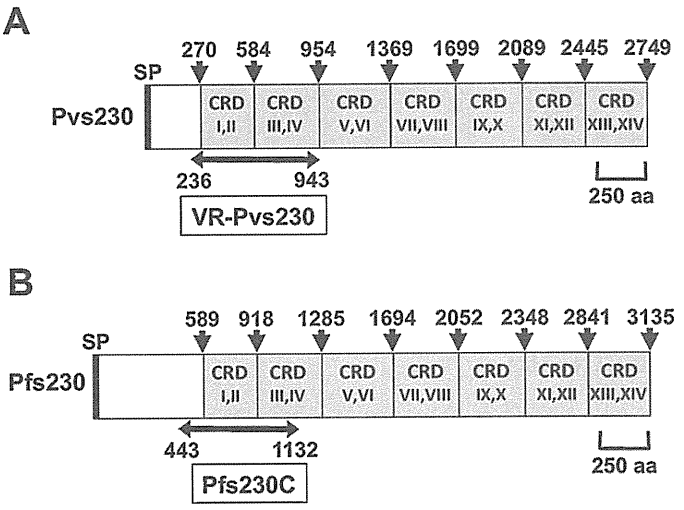


**Fig. 1.** Primary structure of Pvs230 and Pfs230. (A) Target regions for DNA vaccine design and RT-PCR analysis in Pvs230. SP represents signal peptide. The region comprising amino acid positions (aa) 270–2749 consists of the CRD (cysteine-rich domain) I through CRD XIV (regions shaded in gray) as described by Gerloff et al. [15]. Amino acid positions (arrows) 270, 584, 954, 1369, 1699, 2089, 2445, and 2749 indicate the starts of CRD I, III, V, VII, IX, XI, and XIII, respectively. The region that spans the domain I through domain IV (aa 236–943) was used to construct VR-Pvs230 plasmid. (B) Target region utilized for Pfs230 based TBV in the previous study [12]. SP represents a signal peptide. The region comprising amino acid positions (aa) 589–3135 consists of the CRD I through CRD XIV (regions shaded in gray) as described by Gerloff et al. [15]. Amino acid positions (arrows) 589, 918, 1285, 1694, 2052, 2348, 2841, and 3135 represent the starts of CRD I, III, V, VII, IX, XI, and XIII, respectively. Pfs230C indicates the region of Pfs230 that was tested for TBA in the previous study [12].

primer, Pvs230-VR-R1 (5′-ggatcctcaGGTTGCCTCCTGCTTCAACTC-3′) (*Bam*HI restriction site is underlined). Amplified DNA fragment was ligated into the *Bam*HI site downstream of signal sequence of tissue plasminogen activator in a eukaryotic expression vector VR1020 (Vical, Inc., San Diego, CA) to generate VR-Pvs230 plasmid expressing Pvs230 CRDs I–IV. The nucleotide sequence of the insert was confirmed using the Terminator Cycle Sequencing Kit v1.1 (Applied Biosystems, Foster City, CA) in a 310 Genetic Analyzer (Applied Biosystems). The recombinant plasmid was purified using EndoFree Plasmid Maxi Kit (Qiagen, Hilden, Germany). The plasmids were gently mixed with Vaxfectin® (Vical) in the molar ratio of 4:1 as previously described [19,20]. After 10 min incubation at room temperature, the plasmids formulated with Vaxfectin® were administered to mice within 2 h.

### 2.3. Production of anti-Pvs230 serum by DNA immunization

Five female DBA/2 mice in each group were immunized with 50 μg of either VR-Pvs230 (plasmid encoding aa 236–943 of Pvs230) (Fig. 1A) or VR1020 (empty plasmid vector), formulated with adjuvant Vaxfectin® by intradermal injection in the ear pinna 4 times (at 0, 3, 9, and 15 weeks) to produce anti-Pvs230 serum. Mouse antiserum was collected at 17 weeks after initial immunization. The antisera obtained from five mice in each group were pooled, heat inactivated, and stored at −80 °C until use. All animal experimental protocols were approved by the Institutional Animal Care and Use Committee of Ehime University, and the experiments were conducted according to the Ethical Guidelines for Animal Experiments of Ehime University.

### 2.4. Western blot analysis

The parasite proteins were extracted from gametocyte-enriched pellets of *P. vivax* Thai isolates in non-reducing SDS-PAGE loading

buffer, incubated at 95 °C for 3 min, and subjected to electrophoresis on a 7.5% polyacrylamide gel (ATTO, Tokyo, Japan). Proteins were then transferred to a 0.22-μm PVDF membrane (Bio-Rad, Hercules, CA). The membrane was blocked with Blocking One (Nacalai Tesque, Kyoto, Japan), and then incubated with mouse antiserum diluted 1:100 in phosphate buffered saline containing 0.1% Tween 20 (PBST) for 1 h. After washing the blot 3 times in PBST, the membrane was incubated for 30 min with HRP-conjugated goat anti-mouse IgG antibody (Invitrogen) diluted 1:25,000 in PBST. After washing the membrane 3 times with PBST, the proteins on the blot were visualized with Immobilon Western Chemiluminescent HRP Substrate (Millipore, Billerica, MA) on RX-U film (FujiFilm, Tokyo, Japan). The relative molecular mass of the protein was estimated with reference to Precision Plus Protein Standards (BioRad).

### 2.5. Indirect immunofluorescence assay (IFA)

The gametocyte-enriched fraction was spotted onto multiwell slides and acetone-fixed for immunofluorescence assay. The slides were blocked with 5% skimmed milk in PBS at 37 °C for 30 min and incubated with mouse antiserum (1:50) at 37 °C for 1 h. After washing with ice-cold PBS, the slides were incubated with Alexa Fluor® 488 goat anti-mouse IgG (H + L) antibody (1:500; Invitrogen) and nuclear stain 4′,6-Diamidino-2-phenylindole dihydrochloride (DAPI) at 37 °C for 30 min. After washing with ice-cold PBS, the slides were mounted using a ProLong antifade kit (Invitrogen) and images were obtained using fluorescent microscopy (Axiovert200, Carl Zeiss MicroImaging, Thornwood, NY) and confocal scanning laser microscopy (LSM5 Pascal, Carl Zeiss, MicroImaging).

### 2.6. Transmission-blocking assay

Heat-inactivated mouse antiserum was diluted with unheated (complement plus) or heat-inactivated (complement minus) AB+ human serum from malaria naïve Thai volunteers in the ratio of 1:1. These diluted serum samples were then mixed with *P. vivax*-infected erythrocytes from the patients (1:1, v/v ratio) and incubated at room temperature for 15 min. The reconstituted blood samples were introduced into membrane feeders kept at 37 °C. The starved *Anopheles dirus* mosquitoes (Bangkok colony, Armed Forces Research Institute of Medical Sciences, Thailand) were allowed to feed on the sample through the membrane feeder for 30 min. Only fully engorged mosquitoes were maintained for a week with 10% sucrose in the insectary. Twenty mosquitoes for each group were dissected and analyzed by staining with 0.5% Mercurochrome to count the number of oocysts developed within the mosquito midgut under the light microscope. Mann–Whitney *U* test was used to examine the differences in effect on the oocyst counts per mosquito by anti-VR1020 (control) and anti-VR-Pvs230 sera. Infection rate of mosquitoes was calculated as the percentage of oocyst positive mosquitoes out of the total mosquitoes dissected. The difference of the infection rate between control and Pvs230 groups was statistically analyzed by Fisher's exact test. Probability values (*P*) of less than 0.05 were considered statistically significant in both analyses.

### 2.7. Analysis of Polymorphism in Pvs230 CRDs I–IV

DNA fragment encoding Pvs230 CRDs I–IV (aa 236–943) (Fig. 1A) was amplified by PCR from gDNA isolated from *P. vivax* used for the membrane feeding assay with primers designed based on Sal-1 Pvs230 sequence. Primers used are sense Pvs230-30-F (5′-CAGCGATATGGTGATCACC-3′; anneals to nucleotide positions 486–504) and antisense Pvs230-31-R (5′-GCAGGTGTTCTTCACATAGC-3′; anneals to nucleotide positions 2940–2921). For sequencing, the amplified DNA fragment was directly sequenced using the Terminator Cycle Sequencing Kit v1.1 (Applied Biosystems) in a 3100 Genetic Analyzer (Applied Biosystems) as previously described [17].

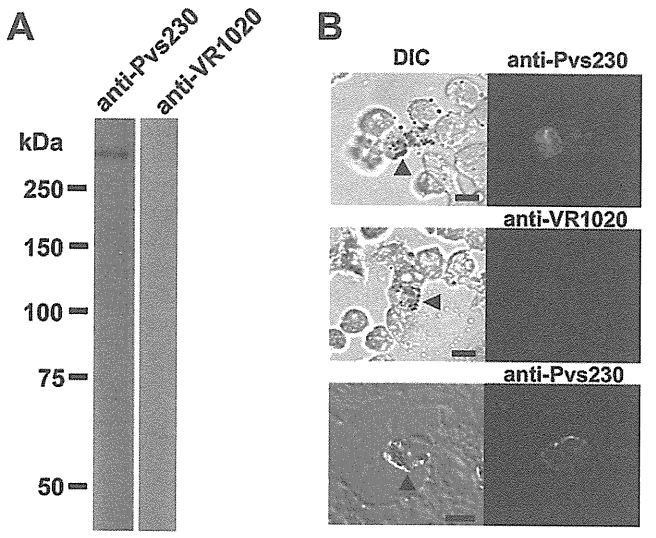


**Fig. 2.** Expression and localization of *pvs230* gene products. (A) Western blot analysis of Pvs230 in the extract from gametocyte-enriched *P. vivax* under non-reducing condition. Lane 1 indicates the probing with mouse anti-Pvs230 serum (anti-Pvs230). Lane 2 indicates the probing with mouse serum produced with an empty plasmid (anti-VR1020) as a negative control. (B) Reactivity of anti-Pvs230 serum by immunofluorescence microscopy. Samples enriched with gametocytes of *P. vivax* were immunostained with anti-Pvs230 serum (top and bottom panels) or antiserum against empty plasmid VR1020 (middle panels). Immunostained images (right panels) were visualized with Alexa Fluor 488-conjugated goat anti-mouse IgG (green). Nuclei were stained with DAPI (blue). The images were obtained with a conventional fluorescence microscope (top and middle panels) or with a confocal microscope (bottom panels). The left panels were the differential interference contrast images (DIC) of the samples in the respective right panels. Gametocytes were marked by arrowheads. The other cells with DAPI-positive nuclei were considered as asexual stage parasites. Scale bars, 5 μm. (For interpretation of the references to color in this figure legend, the reader is referred to the web version of the article.)

## 3. Results

### 3.1. Expression of Pvs230 in the gametocyte of P. vivax

To investigate the protein expression and the localization of Pvs230, mouse antiserum against VR-Pvs230 was generated by DNA immunization. Western blot analyses revealed that mouse anti-Pvs230 serum recognized a high molecular weight band (>250 kDa) in *P. vivax* gametocyte-enriched samples under non-reducing condition (Fig. 2A, lane anti-Pvs230). There was no reactivity of antiserum produced with empty plasmid (Fig. 2A, lane anti-VR1020).

IFA was performed to determine the localization of Pvs230 in the parasite. In fluorescent microscopy, mouse anti-Pvs230 serum specifically reacted with the *P. vivax* gametocyte (Fig. 2B, top panels). In contrast, asexual blood-stage parasites and uninfected erythrocytes did not show any fluorescent signal other than the DAPI nuclear staining (Fig. 2B, top panels). Control serum (VR1020) did not show any reactivity on the parasites and uninfected erythrocytes (Fig. 2B, middle panels). To confirm the localization of Pvs230, the IFA slide was also observed by confocal microscopy. Fluorescence signal was localized on the outer most regions of gametocyte (Fig. 2B, bottom panels) suggesting that Pvs230 might be a surface protein of gametocytes; however further studies involving staining of live parasite is required to confirm the same.

### 3.2. Anti-Pvs230 antibody inhibits transmission of *P. vivax* sample collected from the patient

To evaluate whether mouse anti-Pvs230 serum blocks *P. vivax* transmission to the vector mosquitoes, the transmission-blocking assay was carried out using three *P. vivax* samples collected from three independent Thai patients singly infected with *P. vivax* (Table 1). The results showed that the anti-Pvs230 serum significantly reduced the number of oocysts per midgut formed by all the three *P. vivax* samples both in the presence and absence of complement (Table 1) when compared to the anti-VR1020 serum (control). Moreover, the antiserum significantly reduced the oocyst infection rate when the mosquitoes were fed with sample #1 (with or without complement), and sample #3 (in the absence of complement) (Table 1).

### 3.3. Limited polymorphism in Pvs230 CRDs I–IV

In order to prevent the parasites from evading the immunity induced by vaccines, it is critical to design a vaccine based on protein sequences with minimum polymorphisms. To analyze the extent of polymorphism (i.e., amino acid substitutions) in the DNA vaccine target region (i.e., aa 236–943) of Pvs230 proteins of all the three Thai parasite samples used in our membrane feeding assay, we sequenced region of *Pvs230* encoding aa 236–943 in all the three parasite samples. Among the three parasite specimens, two of them (#2 and #3) had identical amino acid substitutions (i.e., V236F and T743D) as we had reported previously [17]. The sample #1 showed a new amino acid substitution at A484T in addition to V236F and T743D (Fig. 3).

## 4. Discussion

We have demonstrated that a plasmid VR-Pvs230 encoding CRDs I–IV (aa 236–943) of Pvs230 (Fig. 1A) successfully induced the production of mouse antibody that can recognize native Pvs230 protein on the parasite, and significantly reduce the number of oocysts in the mosquito midgut and hence interfere the transmission of *P. vivax* to humans through mosquitoes. This is the first study that demonstrates the expression of Pvs230 protein in the vivax parasite and the transmission-blocking efficacy of anti-Pvs230 serum on *P. vivax*. Despite the fact that VR-Pvs230 was generated from the sequence of *P. vivax* Sal-1 originated from Central America [21], the mouse antibody against VR-Pvs230 efficiently recognized the parasite isolated in Thailand and also reduced its transmission.

A previous study showed that the antibody raised against an *E. coli* expressed N-terminal fragment of Pfs230 denoted as r230/MBP.C [i.e., aa 443–1132, covering upstream pro-domain and CRDs I–III) (Fig. 1B) that is fused with maltose-binding protein (MBP)] recognized the surface of gametes, and reduced the infectivity of *P. falciparum* to mosquitoes in the presence of complement [16]. This was the first demonstration of the transmission-blocking activity by antibody against a recombinant Pfs230 antigen. Therefore, we designed the construct VR-Pvs230 encoding CRDs I–IV of Pvs230 in this study as an initial attempt (Fig. 1A). Since there is no conservation between the pro-domains of Pfs230 and Pvs230 based on the alignment of the deduced amino acid sequences of Pfs230 and Pvs230 [17], we did not incorporate the pro-domain of Pvs230 in our construct.

In a previous report, all of the transmission-blocking monoclonal antibodies against Pfs230 recognized conformational epitopes on the parasite antigen [22]. Owing to the presence of cysteine rich sequences in Pfs230, Pfs230 forms a complicated tertiary structure [15]. This fact indicates that the creation of properly folded conformation of the epitopes of the TBV candidate is critical for the success of transmission-blocking activity. Previously, DNA immunization with a mammalian expression system (Vical plasmid VR1020) was able to generate strong transmission-blocking antibodies for Pfs25 [23], and Pvs25 [24]. A DNA vaccination using a plasmid expressing Pfs230 region C (aa 443–1132) was tried in an attempt to obtain a higher TBA activity than that can be obtained with vaccination using *E. coli*-expressed recombinant protein, r230/MBP.C [25]. Though the antibody titers induced by the Pfs230 region C DNA immunization in mice were measurable, they failed to block transmission [25]. In this study, DNA vaccine (VR-Pvs230) encoding Pvs230 CRDs I–IV was able to induce antibody that recognizes parasite-produced Pvs230 by western blot analysis under non-reducing condition and by IFA, suggesting that the Pvs230 proteins expressed by the DNA vaccine posses at least in part properly folded conformational epitopes. Importantly, anti-Pvs230 antibody raised against the DNA vaccine reduced the oocyst number in the mosquito and interestingly, the reduction was observed both in the presence and absence of active complement (Table 1). The antiserum also reduced the oocyst infection rate when the mosquitoes were fed with sample #1, and with sample #3 (Table 1), however the efficacy measured by the oocyst infection rate appears lower than those measured by oocyst number. Moreover, in sample #2, oocyst number was significantly reduced, but not the oocyst infection rate. These differences are consistent with our recent findings of Pfs230 TBV [12], suggesting that a higher titer of antibody may be required to make oocyst infection rate zero and achieve complete transmission-blocking. The reason for the transmission-blocking activity even in the absence of active complement may be due to the presence of antibody, in the antiserum, that block biological function such as blocking of the fertilization of gametes besides the antibody that is involved in the complement-mediated lysis of gametes. Another possibility

| | Amino acid positions | | | | | | |
|---|---|---|---|---|---|---|---|
| | 236 | 237 | 238 | 300 | 448 | 743 | 789 |
| Sal-1 (reference) | V | V | A | L | A | T | S |
| Thai parasite sample #1 | F | | | | T | D | |
| Thai parasite sample #2 | F | | | | A | D | |
| Thai parasite sample #3 | F | | | | A | D | |
| Previous study on Thai samples [ref. 17] | F | M | D | I/V | | D | N |

**Fig. 3.** Analysis of polymorphism in the region of Pvs230 targeted by DNA vaccine "VR-Pvs230". Nonsynonymous SNP sites in the domain I through IV (encompassing aa 236–943) of Pvs230 proteins of all the three Thai parasite samples used in our membrane feeding assay were analyzed. The numbers refer to the position of amino acids in Pvs230 protein of Sal-1 strain. Only the amino acid substitution sites were indicated. The polymorphism data in Thai vivax samples reported from our previous study [17] was also used for the comparative analysis. Amino acid substitutions found in Thailand were shaded in gray. A newly found substitution site was indicated at amino acid position 484.

**Table 1**
Transmission-blocking effects of the mouse antisera produced by DNA immunization on the parasite specimen from *Plasmodium vivax* cases.

| *P. vivax* sample[a] | Plasmids | Heat inactivation[b] | Oocyst numberMedian (IQR[c]) | $P^d$ | Infection rate(Inf/Diss[e]) | | $P^f$ |
|---|---|---|---|---|---|---|---|
| #1 | VR1020 | Yes | 6.0 (1.75–8.0) | | 85% | 17/20 | |
| | VR-Pvs230 | Yes | 0 (0–0) | <0.0001 | 10% | 2/20 | 0.0039 |
| | VR1020 | No | 9.0 (6.75–10.0) | | 95% | 19/20 | |
| | VR-Pvs230 | No | 0 (0–0.25) | <0.0001 | 25% | 5/20 | 0.0334 |
| #2 | VR1020 | Yes | 3.5 (1.0–12.25) | | 90% | 18/20 | |
| | VR-Pvs230 | Yes | 2.0 (0–4.0) | 0.0436 | 65% | 13/20 | 0.6321 |
| | VR1020 | No | 3.5 (0–8.25) | | 70% | 14/20 | |
| | VR-Pvs230 | No | 0 (0–1.25) | 0.0118 | 45% | 9/20 | 0.4424 |
| #3 | VR1020 | Yes | 4.0 (2.0–7.0) | | 90% | 18/20 | |
| | VR-Pvs230 | Yes | 0 (0–0) | <0.0001 | 20% | 4/20 | 0.0161 |
| | VR1020 | No | 4.0 (1.75–6.25) | | 80% | 16/20 | |
| | VR-Pvs230 | No | 0 (0–0.25) | <0.0001 | 25% | 5/20 | 0.0593 |

[a] Membrane feeding assay was carried out using isolates obtained from three Thai patients singly infected with *P. vivax*.
[b] Heat-inactivated mouse antisera was diluted with unheated (complement plus) or heat-inactivated (complement minus) AB+ human serum from malaria naïve Thai volunteers in the ratio of 1:1.
[c] IQR; inter-quartile range.
[d] For comparing the transmission-blocking effect of Pvs230 immune mouse serum with the matched VR1020-immune mouse serum, the median number of oocyst was statistically analyzed (Mann–Whitney *U* test) and *P*-values less than 0.05 were considered statistically significant.
[e] The oocyst prevalence was calculated by number of oocyst-infected mosquitoes per 20 mosquitoes dissected in each group (Inf/Diss).
[f] Difference between the transmission-blocking effect of Pvs230 and VR1020 immune serum groups was statistically analyzed by Fisher's exact test. *P*-values less than 0.05 were considered statistically significant.

is that the use of Vaxfectin® as adjuvant might have enhanced the titer of Pvs230-specific antibody, for the intramuscular injection of Vaxfectin® formulated with a plasmid DNA encoding influenza nucleoprotein increased antibody titers up to 20-fold, to levels that could not be reached with the plasmid DNA alone [19]. However to validate this claim, we need further studies involving the measurement of antibody titer using properly folded recombinant Pvs230 protein as capture antigen.

In our recent report on the polymorphism of Pvs230, we found 10 amino acid substitutions within the CRDs I–IV (aa 236–943) among isolates worldwide[17]. Six out of 10 amino acid substitutions in comparison with Sal-1 sequence were found in the Thai isolates used in the previous study ($n=20$) [17] (Fig. 3). Among the three parasite specimens used in our membrane feeding assay, two of them (#2 and #3) had identical amino acid substitutions (i.e., V236F and T743D) in the target region (i.e., aa 236–943) of Pvs230. The sample #1 showed a new amino acid substitution at A484T in addition to V236F and T743D (Fig. 3). This analysis shows that the polymorphism in Pvs230 is limited and it may not pose a problem for the utilization of Pvs230 CRDs I–IV as an effective TBV candidate. Further study using larger number of vivax cases is necessary to confirm this preliminary observation about the effect of polymorphism on TBV efficacy.

## Acknowledgments

We thank the staff of the Department of Entomology, Armed Forces Research Institute of Medical Sciences, Bangkok, Thailand, for their technical assistance, and Thangavelu U. Arumugam for the critical reading of the manuscript. We also thank Vical Inc. for providing the VR1020 DNA vaccine plasmid and Vaxfectin® adjuvant. This research was supported in part by the Ministry of Education, Culture, Sports, Science and Technology (21022034, 21249028, 21406010, 23406007), and by the Ministry of Health, Labour, and Welfare, Japan (H21-Chikyukibo-ippan-005).

## References

[1] WHO. World Malaria Report 2010. Geneva, Switzerland: WHO Press; 2010.
[2] Price RN, Tjitra E, Guerra CA, Yeung S, White NJ, Anstey NM. Vivax malaria: neglected and not benign. Am J Trop Med Hyg 2007;77:79–87.
[3] Mueller I, Galinski MR, Baird JK, Carlton JM, Kochar DK, Alonso PL, et al. Key gaps in the knowledge of *Plasmodium vivax*, a neglected human malaria parasite. Lancet Infect Dis 2009;9:555–66.
[4] Kaneko A, Taleo G, Kalkoa M, Yamar S, Kobayakawa T, Bjorkman A. Malaria eradication on islands. Lancet 2000;356:1560–4.
[5] Arevalo-Herrera M, Chitnis C, Herrera S. Current status of *Plasmodium vivax* vaccine. Hum Vaccin 2010;6:124–32.
[6] Herrera S, Bonelo A, Perlaza BL, Fernandez OL, Victoria L, Lenis AM, et al. Safety and elicitation of humoral and cellular responses in Colombian malaria-naive volunteers by a *Plasmodium vivax* circumsporozoite protein-derived synthetic vaccine. Am J Trop Med Hyg 2005;73:3–9.
[7] Malkin EM, Durbin AP, Diemert DJ, Sattabongkot J, Wu Y, Miura K, et al. Phase 1 vaccine trial of Pvs25H: a transmission blocking vaccine for *Plasmodium vivax* malaria. Vaccine 2005;23:3131–8.
[8] Wu Y, Ellis RD, Shaffer D, Fontes E, Malkin EM, Mahanty S, et al. Phase 1 trial of malaria transmission blocking vaccine candidates Pfs25 and Pvs25 formulated with Montanide ISA 51. PLoS ONE 2008;3:e2636.
[9] Kaslow DC, Quakyi IA, Syin C, Raum MG, Keister DB, Coligan JE, et al. A vaccine candidate from the sexual stage of human malaria that contains EGF-like domains. Nature 1988;333:74–6.
[10] Tsuboi T, Kaslow DC, Gozar MM, Tachibana M, Cao YM, Torii M. Sequence polymorphism in two novel *Plasmodium vivax* ookinete surface proteins, Pvs25 and Pvs28, that are malaria transmission-blocking vaccine candidates. Mol Med 1998;4:772–82.
[11] Williamson KC, Criscio MD, Kaslow DC. Cloning and expression of the gene for *Plasmodium falciparum* transmission-blocking target antigen, Pfs230. Mol Biochem Parasitol 1993;58:355–8.
[12] Tachibana M, Wu Y, Iriko H, Muratova O, MacDonald NJ, Sattabongkot J, et al. N-terminal prodomain of Pfs230 synthesized using a cell-free system is sufficient to induce complement-dependent malaria transmission-blocking activity. Clin Vaccine Immunol 2011;18:1343–50.
[13] van Dijk MR, van Schaijk BC, Khan SM, van Dooren MW, Ramesar J, Kaczanowski S, et al. Three members of the 6-cys protein family of *Plasmodium* play a role in gamete fertility. PLoS Pathog 2010;6:e1000853.
[14] Carter R, Coulson A, Bhatti S, Taylor BJ, Elliott JF. Predicted disulfide-bonded structures for three uniquely related proteins of *Plasmodium falciparum*, Pfs230, Pfs48/45 and Pf12. Mol Biochem Parasitol 1995;71:203–10.
[15] Gerloff DL, Creasey A, Maslau S, Carter R. Structural models for the protein family characterized by gamete surface protein Pfs230 of *Plasmodium falciparum*. Proc Natl Acad Sci U S A 2005;102:13598–603.
[16] Williamson KC, Keister DB, Muratova O, Kaslow DC. Recombinant Pfs230, a *Plasmodium falciparum* gametocyte protein, induces antisera that reduce the infectivity of *Plasmodium falciparum* to mosquitoes. Mol Biochem Parasitol 1995;75:33–42.
[17] Doi M, Tanabe K, Tachibana S, Hamai M, Tachibana M, Mita T, et al. Worldwide sequence conservation of transmission-blocking vaccine candidate Pvs230 in *Plasmodium vivax*. Vaccine 2011;29:4308–15.
[18] Han ET, Watanabe R, Sattabongkot J, Khuntirat B, Sirichaisinthop J, Iriko H, et al. Detection of four *Plasmodium* species by genus- and species-specific loop-mediated isothermal amplification for clinical diagnosis. J Clin Microbiol 2007;45:2521–8.
[19] Hartikka J, Bozoukova V, Ferrari M, Sukhu L, Enas J, Sawdey M, et al. Vaxfectin enhances the humoral immune response to plasmid DNA-encoded antigens. Vaccine 2001;19:1911–23.
[20] Sullivan SM, Doukas J, Hartikka J, Smith L, Rolland A. Vaxfectin: a versatile adjuvant for plasmid DNA- and protein-based vaccines. Expert Opin Drug Deliv 2010;7:1433–46.
[21] Collins WE, Contacos PG, Krotoski WA, Howard WA. Transmission of four Central American strains of *Plasmodium vivax* from monkey to man. J Parasitol 1972;58:332–5.

[22] Read D, Lensen AH, Begarnie S, Haley S, Raza A, Carter R. Transmission-blocking antibodies against multiple, non-variant target epitopes of the *Plasmodium falciparum* gamete surface antigen Pfs230 are all complement-fixing. Parasite Immunol 1994;16:511–9.
[23] Lobo CA, Dhar R, Kumar N. Immunization of mice with DNA-based Pfs25 elicits potent malaria transmission-blocking antibodies. Infect Immun 1999;67:1688–93.
[24] Kongkasuriyachai D, Bartels-Andrews L, Stowers A, Collins WE, Sullivan J, Sattabongkot J, et al. Potent immunogenicity of DNA vaccines encoding *Plasmodium vivax* transmission-blocking vaccine candidates Pvs25 and Pvs28-evaluation of homologous and heterologous antigen-delivery prime-boost strategy. Vaccine 2004;22:3205–13.
[25] Fanning SL, Czesny B, Sedegah M, Carucci DJ, van Gemert GJ, Eling W, et al. A glycosylphosphatidylinositol anchor signal sequence enhances the immunogenicity of a DNA vaccine encoding *Plasmodium falciparum* sexual-stage antigen, Pfs230. Vaccine 2003;21:3228–35.

Vaccine 30 (2012) 1972–1980

Contents lists available at SciVerse ScienceDirect

Vaccine

journal homepage: www.elsevier.com/locate/vaccine

# Antibodies against a *Plasmodium falciparum* antigen PfMSPDBL1 inhibit merozoite invasion into human erythrocytes

Hirokazu Sakamoto[a], Satoru Takeo[a], Alexander G. Maier[c,1], Jetsumon Sattabongkot[d,2], Alan F. Cowman[c], Takafumi Tsuboi[a,b,e,*]

[a] *Cell-Free Science and Technology Research Center and Ehime University, Matsuyama, Ehime 790-8577, Japan*
[b] *Venture Business Laboratory, Ehime University, Matsuyama, Ehime 790-8577, Japan*
[c] *The Walter and Eliza Hall Institute for Medical Research, Melbourne, Victoria 3052, Australia*
[d] *Department of Entomology, Armed Forces Research Institute of Medical Sciences, Bangkok 10400, Thailand*
[e] *Ehime Proteo-Medicine Research Center, Ehime University, Toon, Ehime 791-0295, Japan*

ARTICLE INFO

*Article history:*
Received 11 October 2011
Received in revised form 4 January 2012
Accepted 5 January 2012
Available online 14 January 2012

*Keywords:*
Blood-stage vaccine
Merozoite
Malaria
PfMSPDBL1
*Plasmodium falciparum*

ABSTRACT

One approach to develop a malaria blood-stage vaccine is to target proteins that play critical roles in the erythrocyte invasion of merozoites. The merozoite surface proteins (MSPs) and the erythrocyte-binding antigens (EBAs) are considered promising vaccine candidates, for they are known to play important roles in erythrocyte invasion and are exposed to host immune system. Here we focused on a *Plasmodium falciparum* antigen, PfMSPDBL1 (encoded by PF10_0348 gene) that is a member of the MSP3 family and has both Duffy binding-like (DBL) domain and secreted polymorphic antigen associated with merozoites (SPAM) domain. Therefore, we aimed to characterize PfMSPDBL1 as a vaccine candidate. Recombinant full-length protein (rFL) of PfMSPDBL1 was synthesized by a wheat germ cell-free system, and rabbit antiserum was raised against rFL. We show that rabbit anti-PfMSPDBL1 antibodies inhibited erythrocyte invasion of wild type parasites *in vitro* in a dose dependent manner, and the specificity of inhibitory activity was confirmed using PfMSPDBL1 knockout parasites. Pre-incubation of the anti-PfMSPDBL1 antibodies with the recombinant SPAM domain had no effect on the inhibitory activity suggesting that antibodies to this region were not involved. In addition, antibodies to rFL were elicited by *P. falciparum* infection in malaria endemic area, suggesting the PfMSLDBL1 is immunogenic to humans. Our results suggest that PfMSPDBL1 is a novel blood-stage malaria vaccine candidate.



## 1. Introduction

Malaria is a serious infectious disease caused by a protozoan parasite of the genus *Plasmodium*. It causes approximately 300 million illnesses and 1 million deaths annually [1]. The appearance of malaria parasites with resistance to antimalarial drugs and of mosquito vector with resistance to insecticides has highlighted the importance of developing a malaria vaccine. Protective immunity against *Plasmodium falciparum* develops after repeated exposure and prevents severe disease and symptomatic episodes by controlling blood-stage parasitemia [2]. Antibodies are important effectors of protective immunity against malaria as evidenced by experimental animal models and, most importantly, passive transfer studies in which antibodies from malaria-immune adults were successfully used to treat patients with severe malaria [3,4]. These findings provide a strong rationale that an effective vaccine is achievable against the asexual blood-stage parasites by inducing an immune response. Although a number of blood-stage vaccines have been developed and tested in preclinical and clinical trials, only limited clinical success has been achieved with blood-stage vaccines to date [5,6]. Therefore, discovery of novel blood-stage vaccine candidates is an important step towards control of malaria.

One approach to discover a novel malaria vaccine candidate is to target proteins that play critical roles in the invasion process into erythrocytes. The invasion involves multiple steps, including initial attachment, apical reorientation, and tight junction formation, followed by the entry of the merozoite into the erythrocyte. The initial attachment between a free merozoite and an erythrocyte is a reversible interaction and thought to be mediated by merozoite surface proteins (MSPs) [7]. On the other hand, the tight junction formation requires the function of erythrocyte-binding

* Corresponding author at: Cell-Free Science and Technology Research Center, Ehime University, Matsuyama, Ehime 790-8577, Japan. Tel.: +81 89 927 8277; fax: +81 89 927 9941.
*E-mail address:* tsuboi@ccr.ehime-u.ac.jp (T. Tsuboi).
[1] Present address: Department of Biochemistry, La Trobe Institute for Molecular Science, La Trobe University, Melbourne, Victoria 3086, Australia.
[2] Present address: Mahidol Vivax Research Center, Faculty of Tropical Medicine, Mahidol University, Bangkok, Thailand.

0264-410X/$ – see front matter © 2012 Elsevier Ltd. All rights reserved.
doi:10.1016/j.vaccine.2012.01.010

antigens (EBAs). The EBAs are members of the Duffy binding-like (DBL) superfamily, EBA175 (encoded by MAL7P1.176 gene), EBA140/BAEBL (by MAL13P1.160 gene) and EBA181/JESEBL (by PFA0125c gene) are expressed within *P. falciparum* [8]. The EBAs are stored in the micronemes and are secreted onto the merozoite surface just before invasion, and serve as ligands that bind to receptors on the surface of erythrocytes [9–11]. A number of studies have shown that antibodies to these merozoite antigens are thought to function *in vivo* by inhibiting merozoite invasion of erythrocyte (ligand-blocking), opsonizing merozoites for phagocytosis, and inducing antibody-dependent cellular inhibition (ADCI) [12–15]. Since the MSPs and EBAs are exposed to the host immune system, these proteins are considered as promising vaccine candidates and some of these are at various stages of development for clinical trials [16].

Here, we have focused on a novel antigen PfMSPDBL1 (encoded by PF10_0348 gene). This protein has a DBL domain and secreted polymorphic antigen associated with merozoites (SPAM) (Fig. 1A). A previous report [17] showed that the PfMSPDBL1 protein is localized on the merozoite surface and it can bind to the erythrocytes and hence suggested that PfMSPDBL1 may play a role in initial attachment of the erythrocyte by merozoites and that the DBL domain may be a potential target of ligand-blocking antibodies as well as DBL domains of other erythrocyte binding proteins. However, there were not any assays performed in the previous study to prove the invasion inhibitory effect of the anti-PfMSPDBL1 antibodies [17]. On the other hand, recently, a new MSP3 multi-gene family was predicted, and PfMSPDBL1 is one of the members of this family [18]. Because of the high conservation of the MSP3-family in the SPAM domain, antibody against one member cross-reacted to the other MSP3 family members. Importantly, these "cross-reactive" human antibodies inhibited parasite growth in antibody dependent cellular inhibition (ADCI) assays [18]. However, the inhibition was attributed to the "cross-reactive" antibodies, so it is still not known if antibodies that specifically bind to PfMSPDBL1 contributed to this inhibition. In this study, we have investigated the effects of specific antibodies against PfMSPDBL1 protein on erythrocyte invasion by merozoites using growth inhibition assays.

## 2. Materials and methods

### 2.1. Recombinant plasmid construction for protein expression

All recombinant plasmids were constructed using pEU plasmids that are designed specifically for the wheat germ cell-free protein expression system (CellFree Sciences, Matsuyama, Japan) [19]. The nucleotide sequence of the cloned inserts were confirmed using ABI PRISM® 3100-Avant Genetic Analyzer (Applied Biosystems, Foster City, CA). A gene encoding full length [FL, amino acid positions (aa) 26–697] without N-terminal signal peptide of the PfMSPDBL1 (Fig. 1A) and a gene fragment encoding PfMSP1$_{19}$ (aa 1607–1688) were amplified by PCR from the cDNA of *P. falciparum* 3D7 strain. The FL of PfMSPDBL1 gene was cloned into pEU-E01-His-(TEV)-N2 vector between *Xho* I and *Not* I sites (shown in small letters in the primer sequences below), and PfMSP1$_{19}$ gene were cloned into pEU-E01-GST-(TEV)-N2 vector between *Xho* I and *Not* I sites. The nucleotide sequences of the primer pairs used in the PCR amplification were as follows: FL_0076F (5′-ctcgagAATGACCTAATAAATTATAATGATTCGAATCTAAGAAACG-3′), FL_2091R (5′-gcggccgcCTATTTTTGAAATAAATCTGTCATATCTTCTGTCAAACC-3′), msp1-19F (5′-ctcgagATGAACATTTCACAACACCAATGC-3′), msp1-19R (5′-gcggccgcTCAACTGCAGAAAATACCATCGA-3′). To prevent a slippage of RNA polymerase at AT-rich region of *pfmspdbl1* gene and hence potential frame-shift during transcription step, codon optimization was performed using PrimeSTAR® Mutagenesis Basal Kit (Takara, Otsu, Japan) at three regions of adenine-repeat sequences for the FL construct (Fig. 1B). The primer sequences used in the PCR amplifications were as follows: 701–707 bp_F (5′-TAAAG*A*G*AA*G*AA*TCTGAATGCCCTTACAGC-3′), 701–707 bp_R (5′-CAGA*TT*C*TT*C*T*CTTTATAATGTTTCATTAAAGC-3′), 1363–1370 bp_F (5′-TAAC*AA*G*AA*G*AA*TCAAGATTCTCTAACAACC-3′), 1363–1370 bp_R (5′-TGA*TT*C*TT*C*TT*GTTATCAATTACTGCTTTAAG-3′), 1871–1875/1901–1909 bp_F (5′-GTG*A*G*AA*G*AA*G*A*GTATTTCAAAAGTTGACGAAG-3′), 1871–1875/1901–1909 bp_R (5′-TAC*T*C*TT*C*TT*C*T*CACTTTGTTGTTGATTACTGAGTTC*C*TT*C*T*C*CTTA-3′). The italic letters and underlined sequences in the above primers indicate the adenine-repeat sequences and the target bases for codon optimization, respectively. Finally, FL was amplified by PCR from the optimized FL clone, and subcloned into pEU-E01-MCS vector between *Xho* I and *Not* I sites. The primer sequence pair used in the PCR amplification was as follows: FL_atg-0076F (5′-ctcgagATGAATGACCTAATAAATTATAATGATTCGAA-3′), FL_2091R-6His (5′-gcggccgcCTAGTGATGATGATGATGATGTTTTTGAAATAAATCTGTCATATCTTCTGTC-3′). The small letters and underlined sequences in the above primers indicate the restriction site of *Xho* I or *Not* I, and hexa-His tag, respectively.

To express SPAM domains of member of MSP3 family [18], six conserved SPAM domains of the MSP3 family members were amplified by PCR from the cDNA of *P. falciparum* 3D7 strain, and cloned into pEU-E01-His-(TEV)-N2 vector between *Xho* I and *Not* I sites. The primer sequence pairs used in the PCR amplification were as follows: MSP3.1_0499F (5′-ctcgagTATGAAAAGGCAAAAAATGCT-3′), MSP3.1_1065R (5′-gcggccgcTTAATGATTTTTAAAATATTTGGA-3′), MSP3.2_0481F (5′-ctcgagTCTGAAACAAATAAAAATCCTACTTCTCAT-3′), MSP3.2_1116R (5′-gcggccgcTTAATTATTACTAAATAGATGGATCATTTCTTG-3′), MSP3.3_0682F (5′-ctcgagTATGAGAAGAAAAATGAAAATA-3′), MSP3.3_1275R (5′-gcggccgcTTAATTATATGTAAAAAATTCCAT-3′), MSP3.4_1522F (5′-ctcgagGATAATGTAAACTCTGTAACG-3′), MSP3.4_2094R (5′-gcggccgcTTATTTTTGAAATAAATCTGTCAT-3′), MSP3.7_0640F (5′-ctcgagCCTGAAGGACCAAGAGCAAA-3′), MSP3.7_1218R (5′-gcggccgcTCAATAGTTATTTAAAAAAAAAGT-3′), MSP3.8_1609F (5′-ctcgagCATGAAAGTAATGTTGGTAG-3′), MSP3.8_2289R (5′-gcggccgcTTAATTTTTAAATAAATTTGTAAT-3′). The small letters in the above primers indicate the restriction site of *Xho* I or *Not* I.

### 2.2. Production of recombinant proteins and antibodies

We employed the wheat germ cell-free protein expression system (CellFree Sciences) and synthesized recombinant proteins as described previously [20–23]. The recombinant FL protein encompassing the DBL and SPAM domains encoded by amino acids 26–697 was cloned as a C-terminal His-tagged protein (rFL; Fig. 1A) and the six SPAM domains of the MSP3 family members [18] were cloned as N-terminal His-tagged proteins. These proteins were synthesized and purified using Ni-Sepharose column (GE Healthcare, Camarillo, CA). The GST-fused PfMSP1$_{19}$ was captured using Glutathione-Sepharose 4B column (GE Healthcare), and subsequently PfMSP1$_{19}$ was eluted by on-column cleavage with 60 U of AcTEV protease (Invitrogen).

To generate antibodies against rFL, one Japanese white rabbit was immunized subcutaneously with 250 μg of purified proteins with Freund's complete adjuvant, followed by 250 μg with Freund's incomplete adjuvant thereafter. To generate antibodies against PfMSP1$_{19}$, two BALB/c mice were immunized subcutaneously with 30 μg of purified proteins per mouse with Freund's complete adjuvant, followed by 30 μg with Freund's incomplete adjuvant thereafter. All immunizations were done 3 times at 3-week intervals. The antisera were collected 14 days after the last immunization. All animal experimental protocols were approved

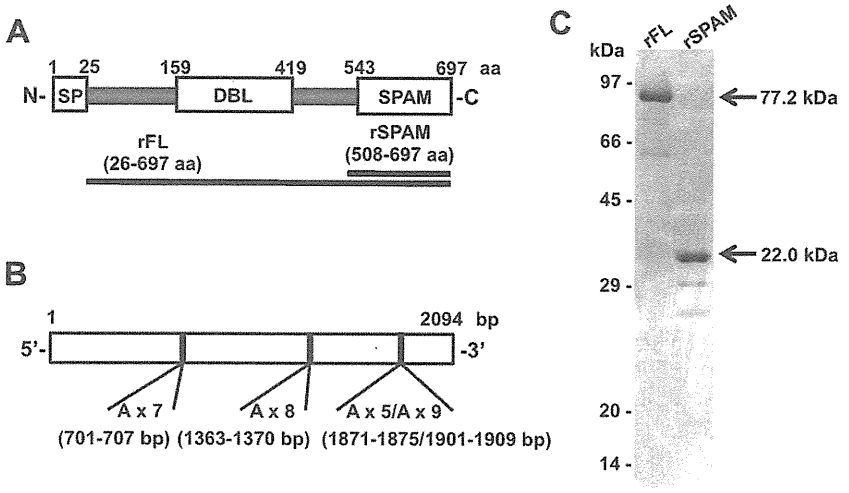


**Fig. 1.** PfMSPDBL1 primary structure, design of constructs, recombinant proteins. (A) Schematic representation of the primary structure of PfMSPDBL1 showing signal peptide (SP, amino acid (aa) 1–25), Duffy binding-like (DBL, aa 159–419) domain and secreted polymorphic antigen associated with merozoites (SPAM, aa 543–697) domain. The black bars highlight the region of the expressed recombinant proteins (rFL, aa 26–697; rSPAM, aa 508–697). (B) The three vertical lines show the codon optimized adenine-rich sites; 7 consecutive adenines, 701–707 bp; 8 consecutive adenines, 1363–1370 bp; 5 and 9 consecutive adenines, 1871–1875 bp and 1901–1909 bp, respectively. The consecutive adenines in these sites were synonymously substituted to guanines by site-directed mutagenesis described in Section 2. (C) SDS-PAGE of recombinant proteins. The purified proteins resolved in a SDS-PAGE and stained with Coomassie brilliant blue R-250 are shown. The two black arrows show purified recombinant FL and SPAM proteins. The arrows show the predicted molecular mass of rFL and rSPAM.

by the Institutional Animal Care and Use Committee of Ehime University, and the experiments were conducted according to the Ethical Guidelines for Animal Experiments of Ehime University.

### 2.3. Parasite culture

The 3D7 strain of *P. falciparum* and the *pfmspdbl1* (PF10_0348) knockout clone of *P. falciparum* (3D7ΔDBL1) (Uboldi et al., in preparation) were maintained in human O+ erythrocytes obtained from the Japanese Red Cross Society as previously described [24]. To harvest parasite pellets, mature schizonts were purified using Percoll (GE Healthcare, Camarillo, CA) density gradient centrifugation and further treated with tetanolysin (List Biological Laboratories, Campbell, CA), washed with phosphate buffered saline (PBS) containing "Complete Protease Inhibitor" (Roche, Mannheim, Germany) and stored at −80 °C until used.

### 2.4. Preparation of the cDNA

Total RNA was extracted from 3D7 parasite-infected erythrocytes rich in schizonts, using Trizol (Invitrogen, Carlsbad, CA) as recommended by the manufacturers and treated with DNase1 (Invitrogen) at 37 °C for 15 min. Superscript III® was used to reverse transcribe DNA-free RNA primed with random hexamer primers (Invitrogen) at 25 °C for 10 min followed by at 50 °C for 50 min and at 85 °C for 5 min.

### 2.5. Western blot analysis

*P. falciparum* native proteins from both 3D7 and 3D7ΔDBL1 parasites rich in schizont were extracted in SDS-PAGE loading buffer and subjected to electrophoresis ($1 \times 10^6$ infected erythrocytes/lane) under reducing condition on a 12.5% polyacrylamide gel (ATTO, Tokyo, Japan). Proteins were transferred to a 0.2 μm PVDF membrane (BioRad, Hercules, CA). After transfer, the membrane was blocked with 5% non-fat milk/PBST (1× PBS/0.1% tween20) at room temperature (RT) for 1 h and probed with anti-rFL serum diluted (1:1000) in PBST. After washing the membrane with PBST, it was incubated with horseradish peroxidase (HRP) conjugated secondary antibodies (GE Healthcare) at RT for 30 min, followed by visualization with Immobilon™ Western Chemiluminescent HRP Substrate (Millipore, Billerica, MA) on LAS 4000 mini luminescent image analyzer (GE Healthcare). The relative molecular sizes of the proteins were calculated with reference to molecular weight size marker "magic mark XP" (Invitrogen).

For cross-reactivity testing for the SPAM domains from MSP3 family members (Fig. 2C), the proteins (100 ng/lane) were subjected to electrophoresis under reducing condition on a 12.5% polyacrylamide gel (ATTO). Western blot analysis was performed as described above. Anti-penta His monoclonal antibody (Qiagen), anti-rFL serum and pooled human sera were used as primary antibodies at 1:500 dilution. The pooled human sera include five individual sera, and a detailed explanation for human sera is given in ELISA section.

### 2.6. Indirect immunofluorescence assay (IFA)

Thin smears of schizont-enriched *P. falciparum* (3D7)-infected erythrocytes were prepared on glass slides and stored at −80 °C. The smears were thawed and fixed with 4% formaldehyde in PBS at RT for 15 min and permeabilized with PBS containing 0.1% Triton X-100 (Nacalai Tesque) at RT for 15 min. The smears were blocked with 5% non-fat milk in PBS at 37 °C for 30 min. They were incubated with primary antibodies [both mouse anti-PfMSP1$_{19}$ serum (1:250 dilution) and rabbit anti-rFL serum (1:500 dilution) antibodies] at 37 °C for 1 h. After washing with PBS, slides were incubated at 37 °C for 30 min with Alexa488-conjugated goat anti-rabbit IgG (Invitrogen; 1:500 dilution), Alexa546-conjugated goat anti-mouse IgG (Invitrogen; 1:500 dilution), and 4′,6-diamidino-2-phenylindole HCl (DAPI, 1 μg/ml; Wako Pure Chemical, Osaka, Japan). The slides were mounted in ProLong Gold antifade reagent (Invitrogen) and examined with LSM710 confocal scanning laser microscope (Carl Zeiss MicroImaging, Thornwood, NY). Images were processed with ImageJ software (National Institutes of Health, Rockville, MD).

### 2.7. Growth inhibition assay

Total IgG to be tested in growth inhibition assays (GIA) was purified from each rabbit antiserum using protein G column (Pierce Inc., Rockford, IL); the purified IgG were dialyzed against RPMI 1640

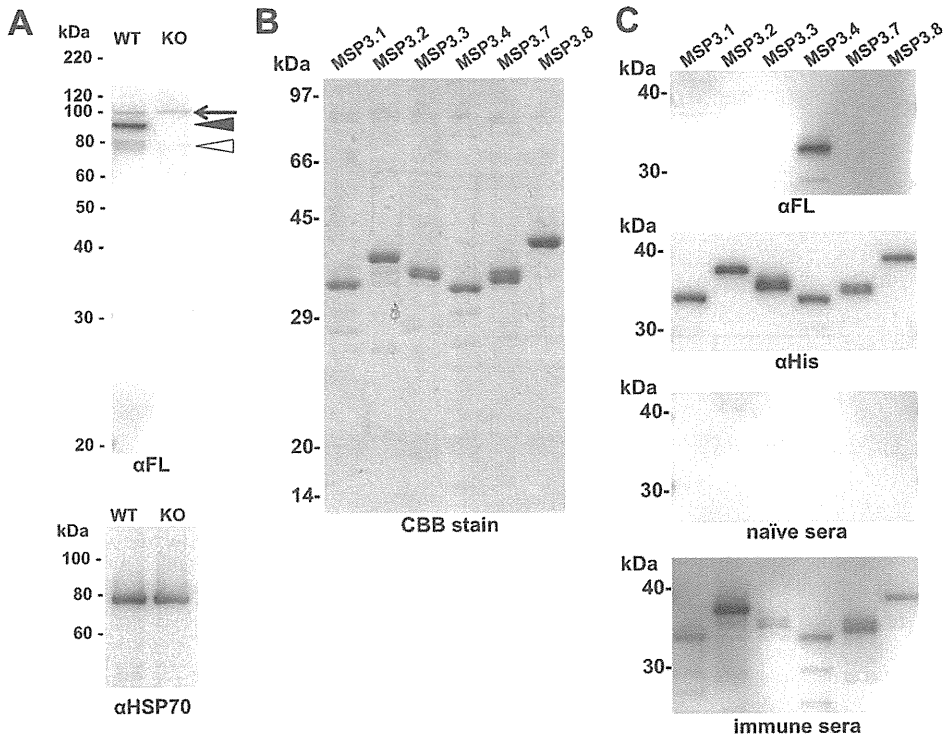


**Fig. 2.** Anti-PfMSPDBL1 antibodies react to native PfMSPDBL1, but not cross-react to SPAM domains of the other MSP3 family members. (A) Western blot analysis of synchronized schizont lysates of 3D7 (WT) and 3D7ΔDBL1 (KO) probed with the anti-rFL polyclonal antiserum (1:1000 dilution) and the anti-PfHSP70 monoclonal antibody (4C9, 1:500 dilution) as a quantitative loading control. The filled arrowhead indicates the full-length form of the native PfMSPDBL1 (95 kDa), the open arrowhead indicates its processed form (80 kDa) and the arrow indicates a nonspecific signal. (B) Recombinant proteins of six conserved SPAM domains of MSP3 family, consisting of MSP3 (MSP3.1), MSP6 (MSP3.2), H101 (MSP3.3), PfMSPDBL1 (MSP3.4), H103 (MSP3.7) and PfMSPDBL2 (MSP3.8) were expressed, and affinity purified. These proteins were separated on 12.5% SDS-PAGE, and stained by Coomassie Brilliant Blue. (C) Western blot analysis of the recombinant SPAM domains probed with anti-rFL serum (top panel), anti-His antibody (second panel), pooled human naïve sera (third panel), or pooled human immune sera (bottom panel).

(Life Technologies, Gaithersburg, MD) and concentrated with an Amicon Ultra-15 30K (Millipore, Billerica, MA) to a concentration of 40 mg/ml or 80 mg/ml. The purified IgGs were reabsorbed with uninfected human O+ erythrocytes (25 μl of RBCs per 1 ml of serum sample) for 1 h at RT with constant rotation to remove any antibodies that specifically binds to human erythrocytes. After reabsorption, IgGs were sterilized by filtration through a 0.22 μm filter (Nalgene Nunc, Rochester, NY) and stored in aliquots at −80 °C.

The growth inhibition assay was performed in a 40 μl culture medium containing human O+ erythrocyte at 1% hematocrit with 0.2–0.4% initial parasitemia in the presence of rabbit IgG in a 96 well half area flat bottom microtiter plate (Corning Incorporated, Corning, NY) at 37 °C for 24–30 h in a humidified, gassed (with 90% $N_2$, 5% $O_2$, and 5% $CO_2$) box. Each IgG was added to a final concentration of 20 mg/ml during setup of the assay, prior to reinvasion. To test the effects of IgGs on growth per se (i.e., for the GIA in Fig. 4C), the IgGs were added to ring stage parasites at 0.2–0.4% initial parasitemia. For the IgG titration growth inhibition assay anti-rFL IgG was added to the well at a final concentration of 0, 1.25, 2.5, 5, 10, or 20 mg/ml. Parasitemia was scored by counting number of infected

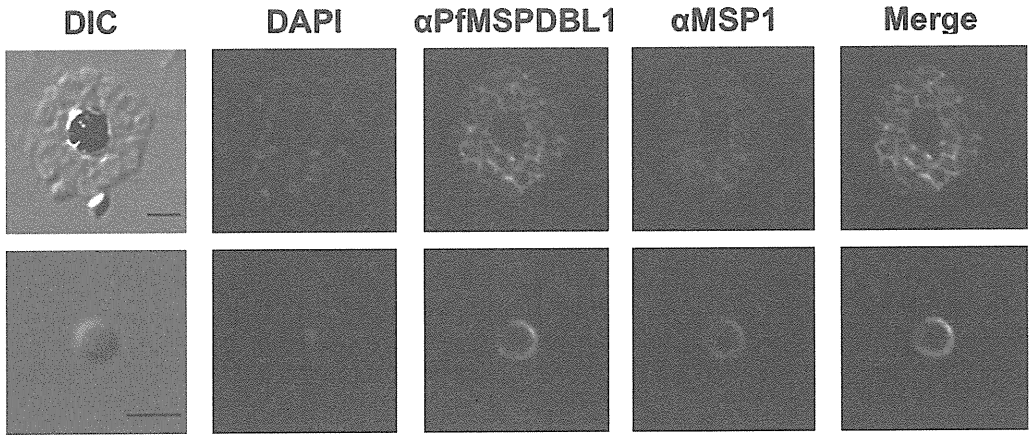


**Fig. 3.** Native PfMSPDBL1 is localized on the merozoite surface. A mature schizont (Triton X-100 permeabilized; upper panel) and a free merozoite (non-permeabilized; bottom panel) of the 3D7 wild type strain were probed with rabbit anti-rFL serum (green) and mouse anti-MSP1 serum (red). Anti-MSP1 was used as a merozoite surface maker. Parasite nuclei were stained with DAPI (blue). Scale bars represent 2 μm. (For interpretation of the references to color in this figure legend, the reader is referred to the web version of the article.)

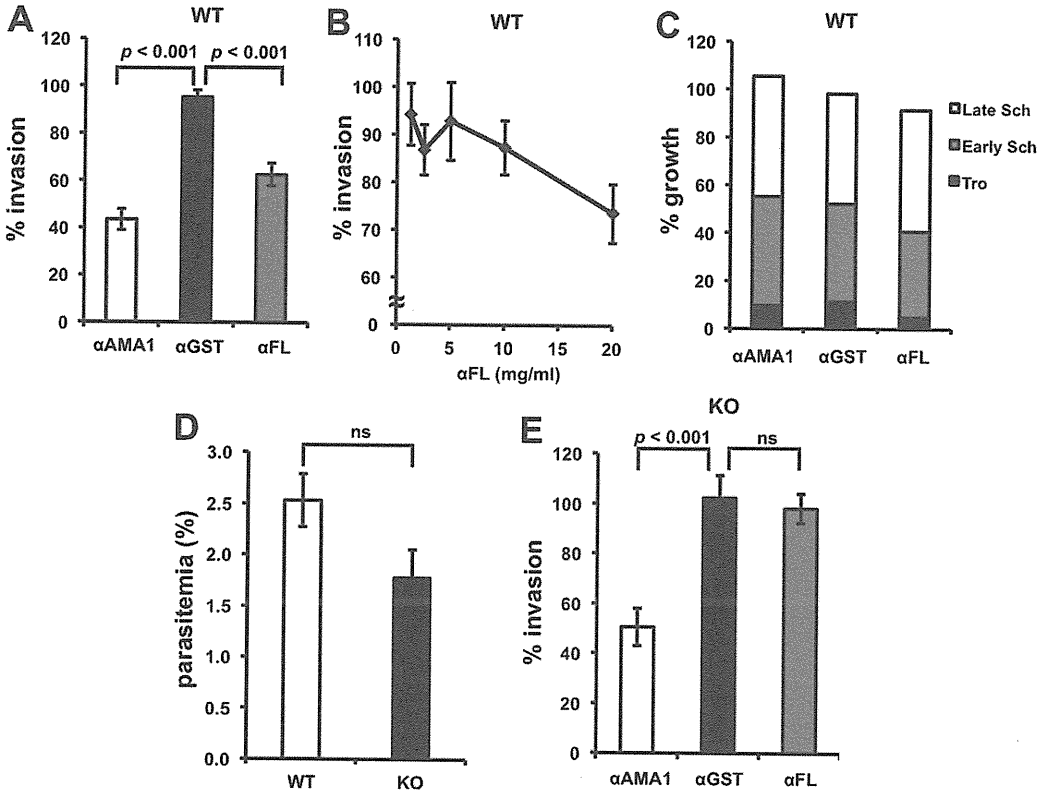


**Fig. 4.** Anti-PfMSPDBL1 antibodies inhibit erythrocyte invasion of merozoites. (A) Anti-rFL IgG have growth inhibitory activity *in vitro*. The ability of the anti-rFL IgG to inhibit invasion and/or growth was tested in one-cycle growth inhibition assay. Anti-AMA1 and anti-GST IgGs were used as positive and negative controls, respectively. Schizonts of 3D7 wild type strain (at 0.2–0.4% initial parasitemia) were cultured in presence of 20 mg/ml of each IgG. One-way ANOVA was performed ($p < 0.001$) followed by Bonferroni's pairwise multiple comparison tests to compare anti-GST and anti-rFL. (B) Percent invasion of the 3D7 wild type strain in the presence of serially diluted anti-rFL IgG. Final concentrations of the IgG were ranged from 0 to 20 mg/ml. (C) Anti-rFL IgG did not affect intra-erythrocytic parasite growth. Rings of 3D7 wild type strain (at 0.2–0.4% initial parasitemia) were cultured in presence of 20 mg/ml of each IgG. Total percent growth and percentage of different stages {i.e., trophozoites (black bar), early schizonts (grey bar), and late schizonts (white bar)} were compared among the three groups. (D) Disruption of *pfmspdbl1* gene do not affect parasite invasion. Post-invasion parasitemia (%) for the 3D7 (WT) and 3D7ΔDBL1 (KO) parasites are shown. Synchronized schizonts of both WT and KO parasites were diluted at 0.2–0.4% initial parasitemia, and then % parasitemia was determined after 30 h of culture. Mean % parasitemia of the three independent experiments were statistically analyzed using Student's *t*-test. (E) The anti-rFL IgG do not inhibit invasion of the 3D7ΔDBL1 parasite. The ability of the anti-rFL IgG to inhibit invasion and/or growth was tested for the 3D7ΔDBL1 parasite in the same manner as shown in Fig. 4A. One-way ANOVA was performed followed by Bonferroni's pairwise multiple comparison tests to compare anti-GST and anti-rFL. For all panels, the error bars represent standard error of the mean (SEM) of three independent experiments.

erythrocytes in 7000 erythrocytes in Giemsa stained thin smears. Each observed parasitemia was divided by the mean value of the parasitemia in three smears of control culture without antibody to give the percent invasion or growth value in each assay. Three independent assays were performed in triplicate.

For the IgG neutralization assay (Fig. 5B), the anti-rFL IgG was incubated with either rFL, rSPAM or rGST protein at 37 °C for 1 h and centrifuged at 4000 × *g* for 3 min, then the supernatant was added to the culture of *P. falciparum*. Final concentrations of IgG and recombinant proteins were at 20 mg/ml and 0.2 mg/ml, respectively. For IgG neutralization using increasing concentration of rFL protein (Fig. 5C), rFL protein at final concentration of either 0, 0.025, 0.05, 0.1, or 0.2 mg/ml was incubated with the anti-rFL IgG (final concentration is at 20 mg/ml). Percent invasion at each point was calculated as described above.

### 2.8. ELISA

All the human serum samples for the determination of antibody against PfMSPDBL1 were collected from adult Thai donors. The serum samples from asymptomatic parasite carriers infected with only *P. falciparum* were collected in the village of Ban Kong Mong Tha, western Thailand with written informed consent [25]. Serum samples were also collected from healthy malaria naïve individuals living in Bangkok, Thailand and used as negative controls. The study was approved by the Ethics Committee of the Thai Ministry of Public Health and the Institutional Review Board of the Walter Reed Army Institute of Research [26]. Measurement of anti-PfMSPDBL1 antibodies in human serum samples was performed according to the standardized ELISA protocol. Briefly, 96-well ELISA plates were coated with 50 ng/well of purified rFL protein at 4 °C overnight in coating buffer (20 mM boric acid, pH 8.9). After the plates were blocked with 2 mg/ml of gelatin in coating buffer, the sera were 1:600 diluted in PBST, added to antigen-coated wells in duplicate, and incubated at 37 °C for 1 h. After washing, the plates were incubated with 1:3000 diluted rabbit anti-human IgG HRP conjugate (DakoCytomation, Glostrup, Denmark) in PBST at 37 °C for 1 h. After washing, the plates were incubated with 0.5 mg/ml azino-bis-3-ethylbenthiazoline-6-sulfonic acid (Wako) diluted in citrate buffer (0.1 M citrate buffer, pH 4.1) at RT for 20 min. The reaction was stopped with 0.1 M citric acid, and optical densities were measured at 415 nm using a precision microplate reader (Molecular Devises, Sunnyvale, CA). Two independent assays were performed in duplicate.

### 2.9. Statistical analysis

The growth inhibition assays were analyzed using a one-way ANOVA test to compare means. If the overall test was significant, Bonferroni's pairwise multiple comparison tests were used to

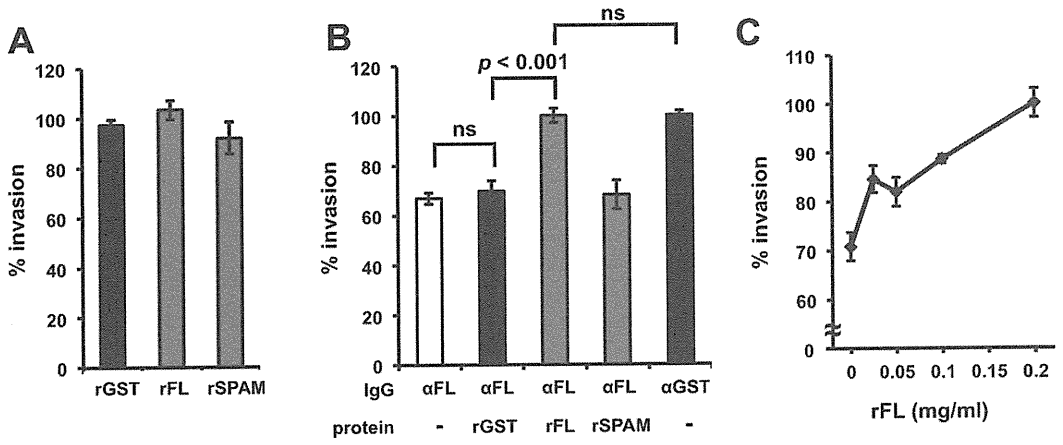


**Fig. 5.** The inhibitory activity of anti-PfMSPDBL1 antibodies is neutralized by the rFL protein, but not rSPAM. (A) Recombinant proteins used for the neutralization did not inhibit parasite invasion. Percent invasion of the parasites for 3D7 strain in the presence of 0.2 mg/ml of each recombinant protein were measured. Statistical analysis was performed using One-way ANOVA and there was no significant difference. (B) The invasion inhibition with the anti-rFL IgG was neutralized by the addition of rFL protein. Percent invasion for the 3D7 strain were determined in the presence of 20 mg/ml of anti-rFL IgG and 0.2 mg/ml of each recombinant protein. Anti-rFL and -GST IgGs (without any recombinant proteins) (–) were used as a positive and a negative control, respectively. Statistical analysis was performed using One-way ANOVA followed by Bonferroni's pairwise multiple comparison tests. (C) Percent invasion of the 3D7 wild type strain in the presence of 20 mg/ml of anti-rFL IgG and rFL protein at increasing concentrations. For all panels, the error bars represent standard error of the mean (SEM) of three independent experiments. For panel B and C, anti-rFL IgG was pre-incubated with recombinant proteins for 1 h and then tested for inhibition.

compare each experimental group to the control. To compare both total percentage growth and ratio of different stages (i.e., trophozoite, early schizont, and late schizont) separately among the three groups in the growth inhibition assay (Fig. 4C) a one-way ANOVA test was performed. To compare the parasitemia in the GIAs using 3D7 wild type and 3D7ΔDBL1 parasites (Fig. 4D), a *F*-test was performed to compare variances, followed by a Student's *t*-test. For an ELISA using human sera (Fig. 6), the antibody responses were not normally distributed and therefore a Mann–Whitney *U*-test was performed comparing medians of the OD values. All statistical analyses were calculated by GraphPad Prism software (GraphPad Software, San Diego, CA).

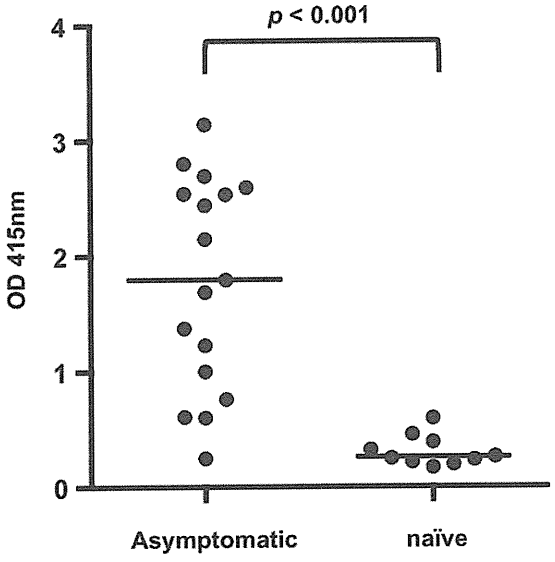


**Fig. 6.** Antibodies to PfMSPDBL1 are elicited in human sera in malaria-endemic area. Antibody responses to rFL in human serum samples were measured with ELISA. The serum samples were obtained from asymptomatic ($n = 17$) or malaria naïve ($n = 10$) adult individuals from malaria-endemic area in Thailand. Two independent assays were performed, and in each assay samples were analyzed in duplicate. Each dot represents the mean of two assays and the bars represent median of each dot. Statistical analysis was performed using the Mann–Whitney *U*-test to compare the medians.

## 3. Results

### 3.1. Synthesis of recombinant PfMSPDBL1 proteins using a wheat germ cell-free system

We designed two recombinant proteins, i.e., rFL and rSPAM of PfMSPDBL1 (Fig. 1A) and expressed them using the wheat germ cell-free system. Fig. 1C shows the recombinant proteins resolved in a 12.5% SDS-polyacrylamide gel. Almost all of the recombinant PfMSPDBL1 proteins were recovered in the soluble fraction and easily purified as a single dominant band (Fig. 1C, arrows) by affinity chromatography. The yields of purified rFL and rSPAM proteins were 73 and 62 μg/6.0 ml of the reaction mixture, respectively. These results demonstrate that the wheat germ cell-free system is able to express PfMSPDBL1 as a soluble protein.

### 3.2. Anti-PfMSPDBL1 antibodies are specific for native PfMSPDBL1

In order to characterize the PfMSPDBL1 protein, a rabbit was immunized with rFL protein. The reactivity of anti-rFL serum was evaluated using schizont-rich parasites by Western blot analysis. To confirm the specificity of the antiserum, lysates of schizont from 3D7 (WT) and the 3D7ΔDBL1 (KO) (Uboldi et al., in preparation) parasites were analyzed (Fig. 2A). Comparison of the reactivity between WT and KO demonstrated that protein bands of approximately 95- (Fig. 2A filled arrowhead) and 80-kDa (Fig. 2A open arrowhead) were specifically detected in the WT but not the KO parasites confirming that the bands identified were specific for PfMSPDBL1. Identification and size of the bands identified was in agreement with previously published results [17]. Preimmune serum did not recognize the native PfMSPDBL1 protein in the lysate of WT parasite (data not shown). To ensure that the same amount of each parasite protein sample was loaded in each lane for Western blot analysis, the membranes were also probed with anti-PfHSP70 monoclonal antibody (4C9) [27]. The intensities of the PfHSP70 bands indicated that the amounts of samples loaded in the lanes were comparable (Fig. 2A, bottom panel). These results suggest that the rFL prepared by the cell-free system retained native epitopes and confirm that anti-rFL serum recognized the native PfMSPDBL1 protein in the 3D7 parasite.

### 3.3. Anti-PfMSPDBL1 antibodies do not cross-react with conserved SPAM domains of other MSP3 family members

Because Singh et al. [18] showed that antibodies against the SPAM domain of the MSP3 family cross-reacts to SPAM domains of other members in MSP3 family, the 100-kDa signal detected in both WT and KO parasites (Fig. 2A arrow) may represent cross-reaction with an unknown MSP3 family member. Therefore we investigated the possibility of the cross-reaction of anti-rFL serum to other SPAM domains of the family. To do this, N-terminal hexa-His-tagged recombinant proteins of all the conserved SPAM domains of the MSP3 family members were synthesized using the wheat germ cell-free system and Ni-affinity purified. The amino acid sequences of different recombinant SPAM domains (Fig. 2B) synthesized by us in this study were identical to that of the respective recombinant SPAM domains synthesized in the previous study [18]. The syntheses of recombinant proteins were confirmed by Coomassie Brilliant Blue staining (Fig. 2B) or anti-His antibody probing in western blotting (second panel of Fig. 2C). To validate antigenicity of the proteins, the SPAM proteins were probed with pooled malaria immune sera (bottom panel of Fig. 2C), or pooled naïve sera from Thailand (third panel of Fig. 2C). All of them reacted to the immune sera (bottom panel of Fig. 2C), but not to the naïve sera (third panel of Fig. 2C), suggesting that all of the recombinant SPAM domains possess correct conformation. However, when these proteins were probed with anti-rFL rabbit serum, none of them except SPAM domain of PfMSPDBL1 reacted against anti-rFL serum indicating that the anti-rFL serum do not cross-react with other conserved SPAM domains of the MSP3 family members, in other words anti-rFL serum react specifically to SPAM domain of PfMSPDBL1 (lane "MSP3.4" in top panel of Fig. 2C).

### 3.4. Native PfMSPDBL1 is localized on the merozoite surface

Although merozoite surface localization of the GFP-fused PfMSPDBL1 protein was previously reported using transgenic parasites [17,28], localization of the native PfMSPDBL1 protein in the parasite, especially free merozoites, has never been confirmed to date. In order to determine the localization of the native PfMSPDBL1 protein in 3D7 wild type mature schizonts and free merozoites, IFA was carried out using anti-rFL and -PfMSP1$_{19}$ sera. In mature schizonts, the PfMSPDBL1 was localized to the circumference of each merozoites (upper panels of Fig. 3). To confirm the surface localization of PfMSPDBL1, we observed the free merozoites that were not permeabilized with Triton X-100. The PfMSPDBL1 was detected on the surface of free merozoites and it was seen to colocalize with PfMSP1 (bottom panels of Fig. 3). On the other hand, under this non-permeabilization condition, the cytoplasmic protein PfHSP70 [probed with anti-PfHSP70 monoclonal antibody (4C9)] was not detected (data not shown), indicating that the parasite plasma membrane is intact. Additionally, in ring and trophozoite stage parasites, PfMSPDBL1 was not detected (data not shown). These results demonstrated for the first time that the native PfMSPDBL1 is localized on the surface of free merozoites and it suggests that it is exposed to human immune system (i.e., neutralizing antibodies).

### 3.5. Anti-PfMSPDBL1 antibodies specifically inhibit merozoite invasion into erythrocytes

To investigate whether anti-rFL antibodies block parasite invasion into erythrocyte, growth inhibition assays were carried out using 3D7 parasites. Anti-AMA1 and -GST IgGs [29,30] were used as a positive and a negative control, respectively. Anti-AMA1 and -GST IgGs inhibited growth by 57% and 5% respectively. Upon culturing parasites with anti-rFL IgG, parasite growth was significantly inhibited (37% inhibition) when compared with anti-GST IgG ($p < 0.001$, Fig. 4A). Moreover, the inhibitory activity of anti-rFL IgG is dose-dependent (Fig. 4B). To test the effects of IgGs on growth per se and not on invasion, the IgGs were added to ring stage parasites at 0.2–0.4% initial parasitemia. After 24–30 h the numbers of intra-erythrocytic parasites (i.e., trophozoites, early schizonts, and late schizonts) were counted. The results showed that among the groups neither total percent growth nor percentage of different stages (i.e., trophozoite, early schizont, and late schizont) were significantly different when the parasites were grown in presence of different IgGs ($p > 0.05$, Fig. 4C). Taken together, anti-rFL IgG inhibits merozoite invasion into erythrocytes but not parasite growth.

To confirm the specificity of the inhibitory activity of the anti-rFL IgG, growth inhibition assays were carried out using the 3D7ΔDBL1 parasite. Before the assay was performed, we compared the invasion efficiency of both wild type 3D7 (WT) and the 3D7ΔDBL1 (KO) parasites (Fig. 4D). Although parasitemia of the 3D7ΔDBL1 was slightly lower than that of the 3D7 wild type parasite after the 30 h observation, the difference in the % parasitemia was not statistically significant (Fig. 4D). Consistent with the data in Fig. 4A, anti-AMA1 IgG significantly inhibited 3D7ΔDBL1 parasite invasion by 50% when compared with anti-GST ($p < 0.001$, Fig. 4E). In contrast, no inhibitory activity of anti-rFL IgG (2% inhibition) was observed when compared with anti-GST ($p > 0.05$). These results indicate that the inhibitory activity of anti-rFL IgG was specific to PfSMSPDBL1 protein.

In order to determine the region of the rFL that is targeted by the inhibitory antibodies, the GIA was performed using anti-rFL IgG that was pre-incubated with either rFL or rSPAM protein. Anti-rFL and -GST IgGs without pre-incubation were used as a positive and a negative control, respectively, and rGST protein was used as a negative control for the pre-incubation. Before performing this assay, we confirmed that all recombinant proteins (final concentration at 0.2 mg/ml) did not have an inhibitory effect on parasite growth (Fig. 5A). As shown in Fig. 5B, the pre-incubation of anti-rFL IgG with rFL protein completely abolished the inhibitory activity of anti-rFL IgG (0% inhibition). Moreover, effect of the pre-incubation on inhibitory activity of anti-rFL IgG was dose-dependent (Fig. 5C). In contrast, pre-incubation of anti-rFL IgG with either rSPAM (32% inhibition) or rGST proteins (30% inhibition) did not reduce the inhibitory activity of anti-rFL IgG (33% inhibition) ($p > 0.05$, Fig. 5B). Taken together, these results suggest that the invasion inhibitory antibodies targets specifically PfMSPDBL1 protein or rather the region of PfMSPDBL1 other than the SPAM domain, and that the antibodies against the SPAM domain did not contribute to the invasion inhibitory activity of anti-rFL IgG.

### 3.6. Antibodies to PfMSPDBL1 were elicited in malaria immune individuals

Since the anti-rFL antibody showed the invasion inhibitory activity, it is important to determine whether PfMSPDBL1 is immunogenic in humans. In order to determine the antibody responses against PfMSPDBL1, serum samples from individuals living in a *P. falciparum* endemic area in Thailand were tested against rFL as capture antigen in ELISA. Malaria naïve human serum samples obtained from individuals living in Bangkok, Thailand were used as a negative control. As shown in Fig. 6, antibody titer against rFL of PfMSPDBL1 was significantly higher in asymptomatic malaria immune sera than in naïve group ($p < 0.001$), suggesting that PfMSPDBL1 was immunogenic to humans.

## 4. Discussion

The striking feature of the PfMSPDBL1 protein is the presence of both DBL and SPAM domains. The well-characterized merozoite